**Referee 1**

*The study presents a new model development and calibration to an interesting horizontally heterogeneous system. It is based on an impressive compiled data set of observations and derivations of relevant inputs and state variables to compare. The main conclusion is that the observed increases in SOM stocks in an agroforest system are due to higher litter input compared to an agricultural control. The modelling exercise is interesting to the soil modelling community, and to the community researching interactions of vegetation components and management. I state several main points followed by more detailed comments.*

**Response:** We thank you for your interest in our work, we really appreciated your comments and suggestions. We tried to take into account all your comments and corrected the manuscript on the requested points.

**NOTE for responses: Pages and lines refer here to the marked-up manuscript version.**

**1 Main points**

*1) One calibration aspect of the study that convinces me (and probably other readers as well) of the validity of the study is currently not well highlighted. The model was calibrated to the control plot only. Despite of simplifying assumptions on similarities in climate and vertical transport between the control and the agroforesty system, the model predicted the differing C-stocks in tree rows and alleys and its depth distribution well. This is a strong validation.*

**Response:** Thanks for this rewarding comment. We better highlighted this result in the abstract "The model was calibrated to the control plot only…The model was strongly validated, describing properly the measured SOC stocks and distribution with depth in agroforestry tree rows and alleys". (P2L30-34), but also in the discussion part "Despite these simplifying assumptions on similarities in climate but also on vertical transport between the control and the agroforestry system, the model calibrated to the control plot was able to reproduce SOC stocks in tree rows and alleys and its depth distribution well. This strong validation also suggests that OC inputs is the main driver of SOC storage, and that a potential effect of agroforestry microclimate on SOC mineralization is of minor importance" (P47L896-902).

*2) The quantification of the priming effect (PE) seems to be a bit complicated with running the no-PE model variant with a decomposition rate that was calibrated with the PE-model variant. To my opinion there are more straightforward quantifications already in the data (see detailed comments). I suggest highlighting the result that the priming model variant in Fig 4 was able to capture the depth distribution of C-stocks while no-PE model variant did not.*

**Response:** We tried to better describe how the PE intensity was quantified (P29-30L635-657) (see below) and why we chose this calculation method. We also highlighted in the abstract the fact that only the PE model was able to describe SOC profiles "Moreover, only a priming effect variant of the model was able to capture the depth distribution of SOC stocks" (P2L36-37).

*3) While the mathematical model is well described, information is missing on the solution of the forward model, i.e. the solution of the presented partial-differential equation given a set of parameters. Which method has been used? What was the spatial grid, the same grid as the measurements? Was this grid sufficient to represent the steep concentration gradient in the top soil? Have different grid sizes been tested?*

**Response:** Partial-differential equations were solved using the R package *deSolve* and the *ode.1D* method (Soetaert et al., 2010) (P28L624-625). The spatial grid was as close as possible to the measurements. Due to some field difficulties, the sampling grid is not totally regular but the modelling grid is. We indeed implicitly assumed this resolution to be sufficient to represent the steep concentration but we did not deeply evaluated the effect of different grid size but if really needed we can provide an analysis in the supplementary material

*4) To my understanding of the study, the increased C stocks at the walnut tree lines are explained in a big part to increase of the above-ground carbon input by the herbaceous summer vegetation between trees (Fig. 3). I would like to read some discussion on this point. Was there an organic layer?*

**Response:** Yes, this is absolutely true, the herbaceous vegetation growing between trees in the tree rows plays an important role on SOC storage. This was very much suggested by previous works on SOC storage in these systems (Cardinael et al., 2015, 2017), but proven here with the quantification of OC inputs. We now discussed this point more into details: "The increased SOC stocks in the tree rows were explained in a big part by an important above-ground carbon input (2.13 t C ha-1 yr-1) by the herbaceous vegetation between trees. This result had already been suggested by Cardinael et al., (2015b) and by Cardinael et al., (2017) who showed that even young agroforestry systems could store SOC in the tree rows while trees are still very small. These "grass strips" indirectly introduced by the tree planting in parallel tree rows have a major impact on SOC stocks of agroforestry systems" (P48L925-931).

As commonly observed on grass strips, there was a very thin organic layer (maximum 0.3 cm thick), but not permanent during the season. Climatic conditions are very favorable for litter decomposition there, and we therefore assumed that this thin organic layer did not significantly change moisture and temperature conditions for the below mineral soil.

## 2 Detailed comments

*L 412: Instead of interpolating parameters of several fits, I suggest fitting a single equation to the entire dataset with an additional variable "distance to tree" and parameters a and b depend on this distance. However, the simplified procedure here seems to work and this point does not affect the conclusions.*

**Response:** Yes, this is indeed another possibility. As we were able to well reproduce root profiles with this simplified method, we think it is not really necessary to look for another equation as it would indeed not change the conclusions.

*L 444: Please specify exactly which observations and which predictions have been used for calibration.*

**Response:** We used SOC stocks measured in 2013 in the control plot (observations) and predicted SOC stocks (predictions) for the calibration. These stocks were considered at equilibrium (P26L568-572).

*Table 7: The prior knowledge in eq. 19 was specified as normal distribution. Table 7 instead reports a range of values instead of a mean and a variance (xb and diagonal of Pb in equation 1). Moreover many ranges span several orders of magnitudes suggesting that the parameters should be log-transformed before estimation. Where does the variance of the posterior come from? And what is the meaning of "prior values" in the posterior column?*

*Table 7: Where did the prior information come from? Are these uninformative priors or does it affect the results if you take different priors?*

**Response:** We acknowledge that this point was not clear enough. The optimization procedure that we used is sensitive to local minima. We therefore performed 30 optimization procedures starting with different parameter prior values to check that the results did not correspond to a local minimum. The prior range presented in Table 7 represents the range in which prior values were sampled for the 30 optimizations, it is therefore normal that they span several orders of magnitudes. The prior values presented in brackets in the posterior column represent the prior values that minimized the **J(x)** value. The variance of the posterior is based on Santaren et al., 2007 (GBC 21, GB2013). The BFGS algorithm does not directly calculate variance of posteriors. To obtain them, we quantified the variance using the curvature cost function at its minimum once it was reached.

We clarified it in the text: "To determine an optimal set of parameters which minimizes J(x), we used the BFGS gradient-based algorithm (Tarantola, 1987). For each model variant, we performed 30 optimizations starting with different parameter prior values to check that the results did not correspond to a local minimum. As the BFGS algorithm does not directly calculate the variance of posteriors, they were quantified using the curvature cost function at its minimum once it was reached (Santaren et al., 2007)." (P27L589-595), and in the Table 7 (now Table 5) footnote: "The prior range represents the range in which prior values were sampled for the 30 optimizations per model variant. The prior values presented in brackets in the posterior column represent the prior values that minimized the J(x) value (Eq. (34))." (P39L824-825).

*Eq 21: Please explain the derivation. Usually the BIC = ln(n)k - 2log(L), which involves the Likelihood instead of the mean squared deviation. From a Bayesian perspective -2log(L) α Jdata(p) , where Jdata is the first term of J of eq. 19 (excluding the prior term).*

**Response:** Here, we used the MSD to estimate the maximum likelihood. This is indeed not the classical BIC. This approach is similar to Manzoni et al., 2012 (SBB 50, 66-76) who used the residual sum of square to estimate the maximum likelihood. We rephrase to clarify: "where $N$ is the number of observations, *MSD* is the mean squared deviation used to estimate the maximum likelihood, and $k$ is the number of model parameters" (P28L604-605).

*L 478: Please, clarify terminology of spin-up vs model calibration. To my understanding you calibrated 4 or 5 parameters depending on the three model variants so that equilibrium stocks,*

*i.e. simulations after 5000 years, were close to observed C-stocks (n=?) of the control plot in 2013. I suggest putting this content to the calibration section.*

**Response:** We moved this paragraph to the optimization procedure section and we clarified the terminology of spin-up vs model calibration: "These four or five parameters were calibrated so that equilibrium SOC stocks, i.e. after 5000 years of simulation, equaled SOC stocks of the control plot in 2013. The associated uncertainty was estimated with the 93 soil cores sampled in the control plot (see section 2.2.1). Due to a lack of relevant data, we assumed that the climate and the land use were the same for the last 5000 years, and that SOC stocks in the control plot were at equilibrium at the time of measurement. Therefore, SOC stocks at the end of the 5000 years of simulation equaled SOC stocks in the control plot. Three different calibrations were performed, corresponding to the three different models that were used: one calibration with the two pools model without the priming effect, one calibration with the two pools model with the priming effect, and one calibration with the three pools model" (P26L564-575). "SOC pools were initialized after a spin-up of 5000 years in the control plot. At $t_0$, SOC stocks in the agroforestry plot therefore equaled SOC stocks of the control plot" (P28L620-622).

*L 508: This derivation of the effect of priming is hard to grasp. To my opinion its more straightforward is compare predictions of the PE-variant model versus the non- PE variant; each consistently calibrated and applied for prediction:*

*• Effects of litter inputs: predictions of no-priming variant only: agroforestry stocks vs control stocks*

*• Combined effect: prediction of the priming model variant only: at agroforestry plot versus the control plot*

*• Effects of priming only: prediction of the priming model variant versus the predictions of the no-priming variant for the agroforestry system*

*Since the profile was not matched well with the no-priming model one can focus on sums.*

**Response:** We agree that the calculation was not straightforward and we clarified it in the new version (see below). Nevertheless, we consider our calculation as the most correct even though it is a bit complex to understand it. Indeed, we can not directly compare the different versions of the model to calculate priming because the decomposition rate of a classical first order kinetics takes implicitly into account a fixed fraction of decomposition due to priming. In all situations, there are regular inputs inducing priming and when we optimized the decomposition rate parameter in the control plot we implicitly represented this priming but at a fixed rate. Therefore comparing the different versions of the model would not estimate the priming in the agroforestry plots.

"Furthermore, at equilibrium state (i.e. when the input rate is constant) the decomposition rate of a first order equation (Eq. (6)) takes *PE* implicitly into account. Indeed, when FOC enters the system, there is an induced priming, a constant FOC input rate therefore induces a constant priming. This means that when we optimized the decomposition rate parameter in the control plot, we implicitly represented this priming but at a fixed rate. When FOC inputs are modified,

due to the tree growth for instance, the PE intensity is modified and this effect cannot be represented by classical first order kinetics." (P29L635-642).

"To estimate the change of SOC decomposition rate due to priming when trees are planted, the decomposition fluxes predicted by Eq. (7) $\left(-k_{HSOC,z} \times (1 - e^{-PE \times FOC_{t,z,d}})\right)$ in the agroforestry plot must be compared to the fluxes in agroforestry plot using the decomposition from the control plot calculated by Eq. (7) with $FOC_{t,z,d}$ corresponding to the FOC inputs in the control plot. Thus, to calculate the importance of priming on SOC storage when trees are planted, we used the decomposition rates calculated following Eq. (7) in the control plot and we applied this decomposition rate to the agroforestry plot as a classical first order kinetics (without the FOC control, i.e. $k_{new} = k_{HSOC,z} \times (1 - e^{-PE \times FOC_{t,z,d}})$ with $FOC_{t,z,d}$ fixed constant)". (P29L642-653).

*Fig 3: Please, note that the largest above ground input comes from herbaceous vegetation. Is this an important aspect for C-stocks of the agroforestry system?*

**Response:** Yes, this is definitely an important aspect for C-stocks in the agroforestry system. We added the following sentence to the result section: "In the agroforestry plot, the largest aboveground OC input to the soil comes from the herbaceous vegetation, and not from the trees" (P28-29L636-637).

*L698 (3.4.2): Please, remind the reader that C-stocks of the agroforestry plot were not part of model calibration (that used the control plot only) but are used here for validation.*

**Response:** As suggested, we added the following sentence at the beginning of the section: **"**As a reminder, SOC stocks of the agroforestry plot were not part of model calibration (that used the control plot only) but were used here for validation" (P36L800-801).

*Fig. 4: This is a nice demonstration of priming formulation being able to match the depth-shape. Although uncertainty of the mean (standard error) is low due to the high sample number, you may add the standard deviation across 93 measurements in order to get an impression of the variability.*

*I would like to see a figure, where C-depth profiles can be compared between cases without being dispersed across facets. Maybe zoom in to 5 to 15 stock range.*

**Response:** Yes, the uncertainty of the mean is extremely low for measured SOC stocks, as suggested we instead added the standard deviation of measurements (P43L857-858).

Concerning the C-depth profiles of Fig 4., this was actually our first idea. But SOC profiles are extremely close, especially between the control and the alleys, and the figure was very messy. We would therefore prefer to stick to this presentation, which is much clearer, even if we have to compare different facets.

*Fig. 5: Please, use a color scale with a clear zero.*

**Response:** We changed the color scale as requested. We also added a 2D graph of modeled control and agroforestry SOC stocks (P44).

*Fig. 6 Please, add difference in measured stocks to the "Inputs+PE" column for comparison.*

**Response:** Thanks for this suggestion, it was done (P46).

*L 753: Suggest: "Despite of these simplifying assumptions, the model calibrated to the control plot was able to ..."*

**Response:** This sentence was changed as follows: "Despite these simplifying assumptions on similarities in climate but also on vertical transport between the control and the agroforestry system, the model calibrated to the control plot was able to reproduce SOC stocks in tree rows and alleys and its depth distribution well. This strong validation also suggests that OC inputs is the main driver of SOC storage at this site, and that a potential effect of agroforestry microclimate on SOC mineralization is of minor importance" (P47L896-902).

**Referee 2**

*This is a comprehensive study that uses an impressive set of field data to build a model for exploring agroforestry impacts on soil organic carbon (SOC). The topic is of interest and fits the scope of the journal. The combination of both field and modeling data is a key strength of this paper and provides interesting results regarding the spatial distribution of SOC in an agroforestry system. The modeling further highlights the potential negative impacts of priming on SOC storage. The methodology, results and most of the interpretation is sound. I therefore recommend this manuscript may be published after addressing the concerns and comments outlined below.*

**Response:** We thank you for your interest and you positive comments on our work.

*Major comments: 1) Due to lack of data, the authors assume that 'soil temperature and soil moisture conditions were the same in the agroforestry tree rows, alleys and in the control plot (L388ff)'. Given the otherwise extensive data collection at this site it is surprising that these key variables have not been measured. As the authors acknowledge at various places, the impact of agroforestry on the SOC is primarily a result of the altered soil abiotic conditions. In my view the lack of these data hamper the understanding of the true controls and mechanisms responsible for change in SOC in the agroforestry system compared to the agricultural control field.*

**Response:** We agree with this comment, it is a pity that soil moisture and soil temperature sensors have not been installed in both fields, and on the long term. But this trial was first established to study crop yield and tree growth in association, and questions on SOC dynamics came very recently. In May 2013 (late Spring, about 15 days after the last rain), we sampled 40 soil cores in the tree rows, 60 in the alleys, and 93 in the control, and we measured soil moisture

on 23 of them. Soil cores were first taken in the agroforestry plot, and then in the control plot, under sunny conditions for both plots. The results showed that soil moisture was lower in the first 40 cm of soil in the control plot, but that there was no difference below:

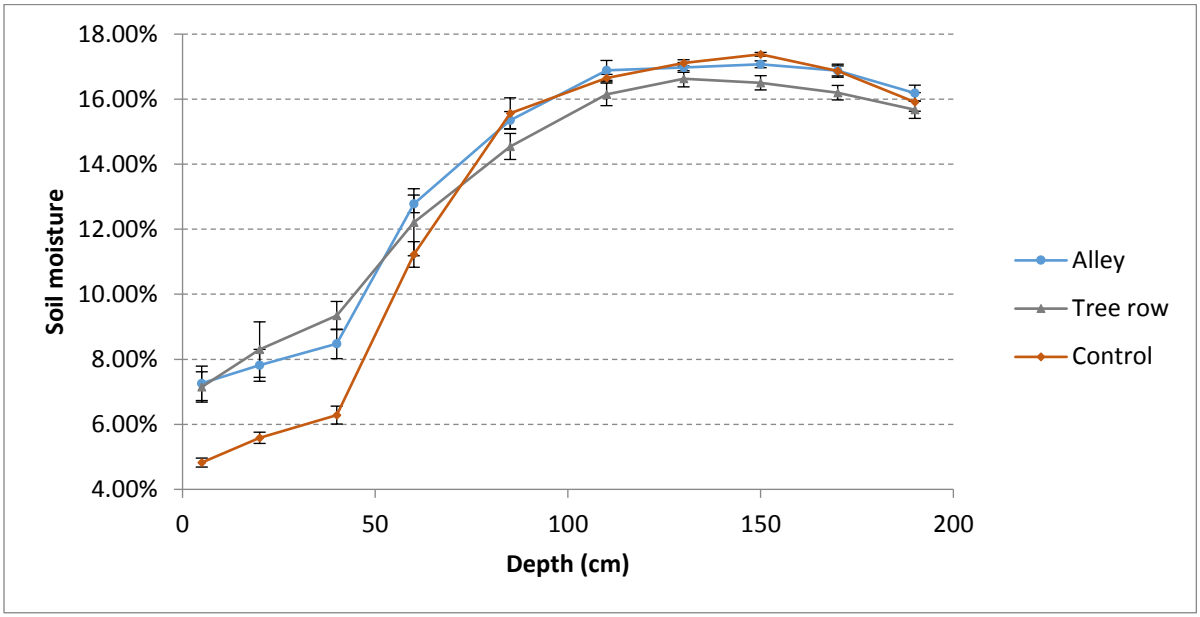


During the last sampling day in the agroforestry plot, some cores were also taken in the control plot, and the same difference in terms of soil moisture was observed, suggesting that the lowest soil moisture in the control plot were not due to the sampling delay. Trees in the agroforestry plot probably slowed down the soil evaporation due to the shade. Most of the additional SOC storage in the agroforestry plot was observed in the topsoil. The lower topsoil soil moisture observed in the control in May 2013 would induce a reduction of SOC decomposition compared to the agroforestry plot, and then would reduce the observed SOC storage. But we can not conclude with this punctual observation, this phenomenon probably alternates during the season. For instance, we could hypothesize that in summer, deep soil will be drier in the agroforestry plot than in the control due to tree water absorption. Due to these uncertainties, we thought it was wiser to consider a mean annual soil temperature and moisture identical in both fields.

*The sensitivity analysis performed by the authors in an attempt to address this limitation cannot replace the missing information on soil abiotic controls since it merely reflects the model sensitivity to these parameters rather than their actual control on SOC. This shortcoming also limits some of the discussion. In my view, the related conclusions that 'that OC inputs is the main driver of SOC storage (L752)', that 'a decrease of SOC mineralization due to the agroforestry microclimate is not obvious (L753)' and that 'soil microclimate in the agroforestry plot are not major drivers of the SOC storage (L766)' are therefore not justified.*

**Response:** We tried to detail but also nuance our conclusions as suggested: "Despite these simplifying assumptions on similarities in microclimate but also on vertical transport between the control and the agroforestry system, the model calibrated to the control plot was able to reproduce SOC stocks in tree rows and alleys and its depth distribution well. This strong validation also suggests that OC inputs is the main driver of SOC storage at this site, and that a

potential effect of agroforestry microclimate on SOC mineralization is of minor importance." (P47L896-902).

"A sensitivity analysis performed on these two boundary conditions showed that the model was not very sensitive to soil temperature and soil moisture (Fig. S4), but the real effect of these two parameters on SOC dynamics under agroforestry systems should be better investigated in future studies" (P48L912-915).

*2) The SOC stock is the product of C concentration per unit soil multiplied by the amount of soil per volume (i.e. bulk density). The study however is entirely focused on explaining changes in SOC due to changes in C concentration (as a result of C input/output) whereas changes in bulk density are not reported. It therefore remains unclear what the separate roles of changes in C concentration and bulk density are in controlling the changes in the total SOC stock (L743ff). While the authors acknowledge that the presence of trees (roots) could modify soil structure (L820), the effects of tree planting on such physical soil properties and subsequently SOC stocks are not well addressed in this study.*

**Response:** This is a very relevant point, soil bulk densities were only lower in the topsoil in the tree rows compared to the alleys and to the control plot. Bulk densities were published earlier (Cardinael et al., 2015b) and thus not reported here. In the model, we used the measured soil bulk densities for the control, tree rows and alleys from Cardinael et al., (2015b) (P8L172). We then expressed SOC stocks on an equivalent soil mass basis, and not at fixed depth. Therefore, the change in bulk density was implicitly taken into account in this study.

*3) The authors argue that the two pools model with priming effect was the best one, as shown by the BICs (Fig. 4, Table S1) (L704). However this is not true for the agroforestry alley which had a similar BIC and RMSE than the noPE model in Fig.4. Since the alley covers most of the area in an agroforesty system, this indicates that the priming effect might be overall less significant for this system as proposed by the authors.*

**Response:** In this case, alleys occupied 84% of the agroforestry area. The BIC and RMSE were lower with the PE model than with the noPE model as indicated in Fig. 4, but we acknowledge the difference is small. In the alleys, the first soil layer (0-10 cm) was worse represented by the PE model than by the noPE model. As the BIC is calculated on the whole profile, this bad fit impacts the BIC even if the PE model performs much better for the other soil layers, this is well shown in Table S2. We therefore think that the PE is need to represent correctly the profile in the alley.

*4) Overall I find that the ms is too long, especially the method section is exhaustive (16 pages incl. Figures and Tables) but also parts of the results could be condensed. Given that the compilation of the C stock data is not a primary study goal (L118ff), I suggest that methods and results related to these data could be considerably shortened and partly moved into the supplementary part or refer to by references. For instance, data shown in Table 4 is already published (Cardinael et al., (2015b) and thus there is no need show this Table once more. Section 3.1 and 3.2, specifically the equations developed here should be moved to the Method*

*or Supplementary section. Details of Section 2.7 could also be moved to the Supplementary part.*

**Response:** We agree that the MS is very long, which is mainly due to the huge amount of data that are compiled here. Moreover, it also includes the differential equations of a new model, which we think are better to be presented in the main manuscript than in the supplementary. We however performed the following changes in order to shorten the description and facilitate comprehension:

Tree fine root biomass data previously shown in Table 4 were moved to the supplementary part (Table S1). Moreover, Section 3.1.1 "Carbon stock in the walnut tree biomass" and Table 3 were deleted as results were already presented in Fig. 3.

Section 3.1.2 "Tree growth" was moved to the Method part and merged with section 2.6.2 "Interpolation of tree growth" (P18L400-403).

Section 3.1.3 "Crop yield" was also moved to the Method part and merged with section 2.6.5 "Aboveground and belowground input from the crop" (P20-24L461-534).

Section 3.2.1"Leaf litterfall" was moved to the Method part and merged with section 2.6.3 "Change of tree litterfall over time" (P18L407-417).

Section 3.2.2 "Tree fine root C input from mortality" was moved to the Method part and merged with section 2.6.4 "Tree fine root C input from mortality" (P19-20L420-458).

Section 3.2.3 "Aboveground carbon input from the crop" and section 3.2.4 were moved to the Method part and merged with section "Aboveground and belowground input from the crop" (P20-24L461-534).

Section 3.2.5 "Aboveground and belowground carbon inputs from the tree row herbaceous vegetation" was moved to the Method part and merged with section 2.6.6 "Aboveground and belowground input from herbaceous vegetation in the tree rows" (P25L541-557).

Section 3.2.6 "Organic carbon inputs and SOC stocks: a synthesis from field measurements" was however kept in the Results (now Section 3.1).

*Minor comments: Line 658: Here and at other places the authors use the word 'globally' which seems inappropriate in the given context.*

**Response:** "Globally" was replace by "Overall" (P36L798 and P40L847).

*L706: 'The spatial distribution of SOC storage was also well described (Fig. 5)' – I disagree, Fig.5 shows the 'additional' SOC in the agroforestry system relative to control but not the absolute amount of SOC storage.*

**Response:** We now also added to Figure 5 both SOC stocks in the control and in the agroforestry plot (P44). This sentence was modified to "The spatial distribution of SOC stocks and of additional SOC storage was also well described (Fig. 5), with a very high additional SOC stock storage in the topsoil layer in the tree row" (P40L849-851).

*L725: 'The priming effect increases the decomposition rate when more FOC is available'– provide a reference for this statement or use past tense to indicate that this is a result from this study.*

**Response:** We added the reference of Fontaine et al., (2007) (P46L870-871).

*L772, 797, 873: At the several places the authors refer to 'the model' while several models (or model variations) were used in this study. Please clarify in each case which of the models (model variation) is meant when referring to one specific model.*

**Response:** We now specified it "the two pools model with priming effect" (P48L923, P49L954 and P52L1031).

*Figure 4: It would be helpful to add separate legends to the middle and right column sub-figures in Fig 4; also how is it possible that the model PE follows the measured SOC profile most closely but results in similar BIC than the noPE model?*

**Response:** As suggested, we added a common legend for all sub-figures at the bottom of Fig 4 (P42). In the alleys, The PE model has almost similar BIC than the noPE model only because the first soil layer (0-10 cm) was worse represented by the PE model: (Model – Measures)^2 = 7.71 compared to 1.28 kg/m3 for the noPE model. As the BIC is calculated on the whole profile, this bad fit impacts the BIC even if the PE model performs much better for the other soil layers, this is well shown in Table S2.

# High organic inputs explain shallow and deep SOC storage in a long-term agroforestry system – Combining experimental and modeling approaches.

Rémi Cardinael[a,b,c*], Bertrand Guenet[d], Tiphaine Chevallier[a], Christian Dupraz[e], Thomas Cozzi[b], Claire Chenu[b]

[a] IRD, UMR Eco&Sols, Montpellier SupAgro, 2 place Viala, 34060 Montpellier, France

[b] AgroParisTech, UMR Ecosys, Avenue Lucien Brétignières, 78850 Thiverval-Grignon, France

[c] CIRAD, UPR AIDA, Avenue d'Agropolis, 34398 Montpellier, France (present address)

[d] Laboratoire des Sciences du Climat et de l'Environnement, UMR CEA-CNRS-UVSQ, CE L'Orme des Merisiers, 91191 Gif-Sur-Yvette, France

[e] INRA, UMR System, Montpellier SupAgro, 2 place Viala, 34060 Montpellier, France

* Corresponding author. Tel.: +33 04.67.61.53.08. E-mail address: remi.cardinael@cirad.fr

*Keywords:* priming effect, deep roots, deep soil organic carbon, spatial heterogeneity, silvoarable system, crop yield, SOC modeling

## Abstract

Agroforestry is an increasingly popular farming system enabling agricultural diversification and providing several ecosystem services. In agroforestry systems, soil organic carbon (SOC) stocks are generally increased, but it is difficult to disentangle the different factors responsible for this storage. Organic carbon (OC) inputs to the soil may be larger, but SOC decomposition rates may be modified owing to microclimate, physical protection, or priming effect from roots, especially at depth. We used an 18-year-old silvoarable system associating hybrid walnut trees (*Juglans regia* × *nigra*) and durum wheat (*Triticum turgidum* L. subsp. *durum*), and an adjacent

agricultural control plot to quantify all OC inputs to the soil - leaf litter, tree fine root senescence, crop residues, and tree row herbaceous vegetation -, and measure SOC stocks down 2 m depth at varying distances from the trees. We then proposed a model that simulates SOC dynamics in agroforestry accounting for both the whole soil profile and the lateral spatial heterogeneity. The model was calibrated to the control plot only.

Measured OC inputs to soil were increased by about 40% (+ 1.11 t C $ha^{-1}$ $yr^{-1}$) down to 2 m depth in the agroforestry plot compared to the control, resulting in an additional SOC stock of 6.3 t C $ha^{-1}$ down to 1 m depth. The model was strongly validated, ~~described~~ describing properly the measured SOC stocks and distribution with depth in agroforestry tree rows and alleys. It showed that the increased inputs of fresh biomass to soil explained the observed additional SOC storage in the agroforestry plot. Moreover, only a priming effect variant of the model was able to capture the depth distribution of SOC stocks. Modeling revealed a strong priming effect that would reduce the potential SOC storage due to higher organic inputs in the agroforestry system by 75 to 90%. This result questions the potential of soils to store large amounts of carbon, especially at depth. Deep-rooted trees modify OC inputs to soil, a process that deserves further studies given its potential effects on SOC dynamics.

## 1 Introduction

Agroforestry systems are complex agroecosystems combining trees and crops or pastures within the same field (Nair, 1993, 1985; Somarriba, 1992). More precisely, silvoarable systems associate parallel tree rows with annual crops. Some studies showed that these systems could be very productive, with a land equivalent ratio (Mead and Willey, 1980) reaching up to 1.3 (Graves et al., 2007). Silvoarable systems may therefore produce up to 30% more marketable biomass on the same area of land compared to crops and trees grown separately. This performance can be explained by a better use of water, nutrients and light by the agroecosystem

51 throughout the year. Trees grown in silvoarable systems usually grow faster than the same trees
52 grown in forest ecosystems, because of their lower density, and because they also benefit from
53 the crop fertilization (Balandier and Dupraz, 1999; Chaudhry et al., 2003; Chifflot et al., 2006).
54 In temperate regions, farmers usually grow one crop per year, and this association of trees can
55 extend the growing period at the field scale, especially when winter crops are intercropped with
56 trees having a late bud break (Burgess et al., 2004). However, after several years, a decrease of
57 crop yield can be observed in mature and highly dense plantations, especially close to the trees,
58 due to competition between crops and trees for light, water, and nutrients (Burgess et al., 2004;
59 Dufour et al., 2013; Yin and He, 1997).
60 Part of the additional biomass produced in agroforestry is used for economical purposes, such
61 as timber or fruit production. Leaves, tree fine roots, pruning residues and the herbaceous
62 vegetation growing in the tree rows will usually return to the soil, contributing to a higher input
63 of organic carbon (OC) to the soil compared to an agricultural field (Peichl et al., 2006).
64 In such systems, the observed soil organic carbon (SOC) stocks are also generally higher
65 compared to a cropland (Albrecht and Kandji, 2003; Kim et al., 2016; Lorenz and Lal, 2014).
66 Cardinael *et al.*, (2017) measured a mean SOC stock accumulation rate of 0.24 (0.09-0.46) t C
67 $ha^{-1}$ $yr^{-1}$ at 0-30 cm depth in several silvoarable systems compared to agricultural plots in
68 France. Higher SOC stocks were also found in Canadian agroforestry systems, but measured
69 only to 20 cm depth (Bambrick et al., 2010; Oelbermann et al., 2004; Peichl et al., 2006).
70 To our knowledge, we are still not able to disentangle the factors responsible for such a higher
71 SOC storage. This SOC storage might be due to higher OC inputs but it could also be favored
72 by a modification of the SOC decomposition owing to a change in SOC physical protection
73 (Haile et al., 2010), and/or in soil temperature and moisture.
74 The introduction of trees in an agricultural field modifies the amount, but also the distribution
75 of fresh organic carbon (FOC) input to the soil, both vertically and horizontally (Bambrick et

al., 2010; Howlett et al., 2011; Peichl et al., 2006). FOC inputs from the trees decrease with increasing distance from the trunk and with soil depth (Moreno et al., 2005). On the contrary, crop yield usually increases with increasing distance from the trees (Dufour et al., 2013; Li et al., 2008). Therefore, the proportions of FOC coming from both the crop residues and the trees change with distance from the trees, soil depth, and time.

Tree fine roots (diameter $\leq 2$ mm) are the most active part of root systems (Eissenstat and Yanai, 1997) and play a major role in carbon cycling. In silvoarable systems, tree fine root distribution within the soil profile is strongly modified due to the competition with the crop, inducing a deeper rooting compared to trees grown in forest ecosystems (Cardinael et al., 2015a; Mulia and Dupraz, 2006). Deep soil layers may therefore receive significant OC inputs from fine root mortality and exudates. Root carbon has a higher mean residence time in the soil compared to shoot carbon (Kätterer et al., 2011; Rasse et al., 2006), presumably because root residues are preferentially stabilized within microaggregates or adsorbed to clay particles. Moreover, temperature and moisture conditions are more buffered in the subsoil than in the topsoil. The microbial biomass is also smaller at depth (Eilers et al., 2012; Fierer et al., 2003), and the spatial segregation with organic matter is larger (Salomé et al., 2010) resulting in lower decomposition rates. Deep root carbon input in the soil could therefore contribute to a SOC storage with high mean residence times. However, some studies showed that adding FOC – a source of energy for microorganisms - to the subsoil enhanced decomposition of stabilized carbon, a process called « priming effect » (Fontaine et al., 2007). The priming effect is stronger when induced by labile molecules like root exudates than by root litter coming from the decomposition of dead roots (Shahzad et al., 2015). Therefore, the net effect of deep roots on SOC stocks has to be assessed, especially in silvoarable systems.

Models are crucial as they allow virtual experiments to best design and understand complex processes in these systems (Luedeling et al., 2016). Several models have been developed to

simulate interactions for light, water and nutrients between trees and crops (Charbonnier et al., 2013; Duursma and Medlyn, 2012; van Noordwijk and Lusiana, 1999; Talbot, 2011) or to predict tree growth and crop yield in agroforestry systems (Graves et al., 2010; van der Werf et al., 2007). However, none of these models are designed to simulate SOC dynamics in agroforestry systems and they are therefore not useful to estimate SOC storage. Oelbermann & Voroney (2011) evaluated the ability of the CENTURY model (Parton et al., 1987) to predict SOC stocks in tropical and temperate agroforestry systems, but with a single-layer modeling approach (0-20 cm). The approach of modeling a single topsoil layer assumes that deep SOC does not play an active role in carbon cycling, while it was shown that deep soil layers contain important amounts of SOC (Jobbagy and Jackson, 2000), and that part of this deep SOC could cycle on decadal timescales due to root inputs or to dissolved organic carbon transport (Baisden and Parfitt, 2007; Koarashi et al., 2012). The need to take into account deep soil layers when modeling SOC dynamics is now well recognized in the scientific community (Baisden et al., 2002; Elzein and Balesdent, 1995), and several models have been proposed (Braakhekke et al., 2011; Guenet et al., 2013; Koven et al., 2013; Taghizadeh-Toosi et al., 2014; Ahrens et al., 2015). Using vertically discretized soils is particularly important when modeling the impact of agroforestry systems on SOC stocks, but to our knowledge, vertically spatialized SOC models have not yet been tested for these systems.

The aims of this study were then twofold: (i) to propose a model of soil C dynamics in agroforestry systems able to account for both vertical and lateral spatial heterogeneities and (ii) to test whether variations of fresh organic carbon (FOC) input could explain increased SOC stocks both using experimental data and model runs.

For this, we first compiled data on FOC inputs to the soil obtained in a 18-year-old agroforestry plot and in an agricultural control plot in southern France, in which SOC stocks have been

recently quantified to 2 m depth (Cardinael et al., 2015b). FOC inputs comprised tree fine roots, tree leaf litter, aboveground and belowground biomass of the crop and of the herbaceous vegetation in the tree rows. We compiled recently published data for FOC inputs (Cardinael et al., 2015a; Germon et al., 2016), and measured the others (Table 1).

We then modified a two pools model proposed by Guenet *et al.*, (2013), to create a spatialized model over depth and distance from the tree, the CARBOSAF model (soil organic CARBOn dynamics in Silvoarable AgroForestry systems). Based on data acquired since the tree planting in 1995 (crop yield, tree growth), and on FOC inputs, we modeled SOC dynamics to 2 m depth in both the silvoarable and agricultural control plot. We evaluated the model against measured SOC stocks along the profile and used this opportunity to test the importance of priming effect (*PE*) for deep soil C dynamics in a silvoarable system. The performance of the two pools model including *PE* was also compared with a model version including three OC pools.

## 2 Materials and methods

### 2.1 Study site

The experimental site is located at the Restinclières farm Estate in Prades-le-Lez, 15 km North of Montpellier, France (longitude 04°01' E, latitude 43°43' N, elevation 54 m a.s.l.). The climate is sub-humid Mediterranean with an average temperature of 15.4°C and an average annual rainfall of 973 mm (years 1995–2013). The soil is a silty and carbonated (pH = 8.2) deep alluvial Fluvisol (IUSS Working Group WRB, 2007). In February 1995, a 4.6 hectare silvoarable agroforestry plot was established with the planting of hybrid walnut trees (*Juglans regia* × *nigra* cv. NG23) at a density of 192 trees $ha^{-1}$ but later thinned to 110 trees $ha^{-1}$. Trees were planted at 13 m × 4 m spacing, and tree rows are East–West oriented. The cultivated alleys are 11 m wide. The remaining part of the plot (1.4 ha) was kept as an agricultural control plot.

Since the tree planting, the agroforestry alleys and the control plot were managed in the same way. The associated crop is most of the time durum wheat (*Triticum turgidum* L. subsp. *durum*), except in 1998, 2001 and 2006, when rapeseed (*Brassica napus* L.) was cultivated, and in 2010 and 2013, when pea (*Pisum sativum* L.) was cultivated. The soil is ploughed to a depth of 0.2 m before sowing, and the wheat crop is fertilized with an average of 120 kg N $ha^{-1}$ $yr^{-1}$. Crop residues (wheat straw) are also exported, but about 25% remain on the soil. Tree rows are covered by spontaneous herbaceous vegetation. Two successive herbaceous vegetation types occur during the year, one in summer and one in winter. The summer vegetation is mainly composed of *Avena fatua* L., and is 1.5 m tall. In winter, the vegetation is a mix of *Achillea millefolium* L., *Galium aparine* L., *Vicia* L., *Ornithogalum umbellatum* L. and *Avena fatua* L, and is 0.2 m tall.

**Table 1.** Synthesis of the different field and laboratory data available or measured, and their sources.

| Description of the data | Source |
|---|---|
| Soil texture, bulk densities, SOC stocks | Cardinael *et al.*, (2015a) |
| Soil temperature and soil moisture | Measured |
| Tree growth (DBH) | Measured |
| Tree wood density | (Talbot, 2011) |
| Tree fine root biomass | Cardinael *et al.*, (2015b) |
| Tree fine root turnover | Germon *et al.*, (2016) |
| Crop yield and crop ABG biomass | Dufour *et al.*, (2013) and measured |
| Crop root biomass | Prieto *et al.*, (2015) and measured |
| Tree row herbaceous vegetation – ABG biomass | Measured |
| Tree row herbaceous vegetation – root biomass | Measured |
| Biomass carbon concentrations | Measured |
| Potential decomposition rate of roots | Prieto *et al.*, (2016a) |
| HSOC potential decomposition rate | Measured |

DBH: Diameter at Breast Height; ABG: aboveground; OC: organic carbon; HSOC: humified soil organic carbon.

## 2.2 Organic carbon stocks

### 2.2.1 Soil organic carbon stocks

SOC data have been published in Cardinael *et al.*, (~~2015a~~2015b). Briefly, soil cores were sampled down to 2 m depth in May 2013, 100 in the agroforestry plot, and 93 in the agricultural control plot. SOC concentrations, soil bulk densities, SOC stocks, and soil texture were measured for ten soil layers (0.0-0.1, 0.1-0.3, 0.3-0.5, 0.5-0.7, 0.7-1.0, 1.0-1.2, 1.2-1.4, 1.4-1.6, 1.6-1.8, and 1.8-2.0 m). In the agroforestry plot, 40 soil cores were taken in the tree rows, while 60 were sampled in the alleys at varying distances from the trees. Soil organic carbon stocks were quantified on an equivalent soil mass basis (Ellert and Bettany, 1995).

### 2.2.2 Tree aboveground and stump carbon stocks

Three hybrid walnuts were chopped down in 2012. The trunk circumference was measured every meter up to the maximum height of the tree to estimate its volume. The trunk biomass was estimated by multiplying the trunk volume by the wood density that was measured at 616 kg $m^{-3}$ during a previous work at the same site (Talbot, 2011). Then, branches were cut, the stump was uprooted, and they were weighted separately. Samples were brought to the laboratory to determine the moisture content, which enabled calculation of the branches and the stump dry mass.

## 2.3 Measurements of organic carbon inputs in the field

### 2.3.1 Carbon inputs from tree fine root mortality

The tree fine root (diameter ≤ 2 mm) biomass was quantified and coupled with an estimate of the tree fine root turnover in order to predict the carbon input to the soil from the tree fine root mortality. A detailed description of the methods used to estimate the tree fine root biomass can be found in Cardinael *et al.*, (~~2015b~~2015a). In March 2012, a 5 (length) × 1.5 (width) × 4 m (depth) pit was open in the agroforestry plot, perpendicular to the tree row, at the North of the

trees. The tree fine root distribution was mapped down 4 m depth, and the tree fine root biomass was quantified in the tree row and in the alley. Only results concerning the first two meters of soil, among those obtained by Cardinael *et al.*, (~~2015b~~2015a) will be ~~presented~~ used here.

In July 2012, sixteen minirhizotrons were installed in the agroforestry pit, at 0, 1, 2.5 and 4 m depth, and at two and five meters from the trees. The tree root growth and mortality was monitored during one year using a scanner (CI-600 Root Growth Monitoring System, CID, USA), and analyzed using the WinRHIZO Tron software (Régent, Canada). A detailed description of the methods and of results used to estimate the tree fine root turnover can be found in Germon *et al.*, (2016).

### 2.3.2 Tree litterfall

In 2009, the crowns of two walnut trees were packed with a net in order to collect the leaf biomass from September to January. The same was done in 2012 with three other walnut trees. The leaf litter was then dried, weighted and analyzed for C to quantify the leaf carbon input per tree.

### 2.3.3 Aboveground and belowground input from the crop

Since the tree planting in 1995, the crop yield was measured 14 times (in 1995, 2000, 2002, 2003, 2004, 2005, 2007, 2008, 2009, 2010, 2011, 2012, 2013, and 2014), while the wheat straw biomass and the total aboveground biomass were measured six times (in 2007, 2008, 2009, 2011, 2012, and 2014) in both the control and the agroforestry plot (Dufour et al., 2013), using sampling subplots of 1 $m^2$ each. In the control plot, five subplots have been sampled while in the agroforestry plot five transects have been sampled. Each transect was made of three subplots, 2 m North from the tree, 2 m South from the tree, and 6.5 m from the tree (middle of the alley). In March 2012, a 2 m deep pit was opened in the agricultural control plot (Prieto et

al., 2015), and the root biomass was quantified to the maximum rooting depth (1.5 m). The root:shoot ratio of durum wheat was measured in the control plot. We assumed that the crop root biomass turns out once a year, after the crop harvest.

### 2.3.4 Above and belowground input from the tree row herbaceous vegetation

As two types of herbaceous vegetation grow in the tree rows during the year, samples were taken in summer and winter. In late June 2014, twelve subplots of 1 $m^2$ each were positioned in the tree rows, around 4 walnut trees. In January 2015, six subplots of 1 $m^2$ each were positioned in the tree rows, around 2 walnut trees. The middle of each subplot was located at 1 m, 2 m and 3 m, respectively, from the selected walnut tree. All the aboveground vegetation was collected in each square. In the middle of each subplot, root biomass was sampled with a cylindrical soil corer (inner diameter of 8 cm). Soil was taken at three soil layers, 0.0-0.1, 0.1-0.3 and 0.3-0.5 m. In the laboratory, soil was gently washed with water through a 2 mm mesh sieve, and roots were collected. Roots from the herbaceous vegetation were easily separated manually from walnut roots, as they were soft and yellow compared to walnuts roots that were black. After being sorted out from the soil and cleaned, the root biomass was dried at 40°C and measured.

## 2.4 Carbon concentration measurements

All organic carbon measurements were performed with a CHN elemental analyzer (Carlo Erba NA 2000, Milan, Italy), after samples were oven-dried at 40°C for 48 hours (Table 2). Dry biomasses (t DM $ha^{-1}$) of each organic matter inputs were multiplied by their respective organic carbon concentrations (mg C $g^{-1}$) to calculate organic carbon stocks (t C $ha^{-1}$).

**Table 2.** Organic carbon concentrations and C:N ratio of the different types of biomass.

| Type of biomass | Organic C concentration (mg C $g^{-1}$) | C:N | Number of replicates |
|---|---|---|---|
| Walnut trunk | 445.7 ± 1.0 | 159.1 ± 25.2 | 3 |
| Walnut branches | 428.6 ± 1.7 | 62.2 ± 11.7 | 3 |
| Wheat straw | 433.2 ± 0.7 | 55.5 ± 2.1 | 5 |
| Wheat root | 351.4 ± 19 | 24.8 ± 2.1 | 8 |
| Walnut leaf | 449.4 ± 3.7 | 49.1 ± 0.4 | 3 |
| Walnut fine root | 437.0 ± 3.3 | 28.6 ± 3.4 | 8 |
| Summer vegetation (ABG) | 448.4 ± 1.9 | 37.8 ± 2.2 | 5 |
| Summer vegetation (roots) | 314.5 ± 8.3 | 33.8 ± 1.7 | 6 |
| Winter vegetation (ABG) | 447.7 ± 5.3 | 11.2 ± 0.4 | 3 |
| Winter vegetation (roots) | 397.4 ± 5.0 | 24.7 ± 0.7 | 3 |

The organic matter called "vegetation" stands for the herbaceous vegetation that grows in the tree row. ABG: aboveground. Errors represent standard errors.

## 2.5 General description of the CARBOSAF model

### 2.5.1 Organic carbon decomposition

We adapted a model developed by Guenet et al. (2013) where total SOC is split in two pools, the FOC and the humified soil organic carbon (HSOC) for each soil layer (Fig. 1a). Input to the FOC pool comes from the plant litter and the distribution of this input within the profile is assumed to depend upon depth from the surface ($z$), distance from the tree ($d$), and time ($t$). Equations describing inputs to the FOC pool ($I_{t,z,d}$) at a given time, depth, and distance are fully explained in the Results.

The FOC mineralisation is assumed to be governed by first order kinetics, being proportional to the FOC pool, as given by:

$$\frac{\partial FOC_{t,z,d}}{\partial t} = -k_{FOC} \times FOC_{t,z,d} \times f_{clay,z} \times f_{moist,z} \times f_{temp,z} \qquad (1)$$

where $FOC_{t,z,d}$ is the FOC carbon pool (kg C $m^{-2}$) at a given time ($t$, in years), depth ($z$, in m) and distance ($d$, in m), and $k_{FOC}$ is its decomposition rate. The potential decomposition rates of the different plant materials were assessed with a 16-week incubation experiment during a companion study at the site (Prieto et al., 2016). The decomposition rate $k_{FOC}$ was weighted by

the respective contribution of each type of plant litter as a function of the tree age, soil depth and distance from the tree. The rate modifiers $f_{clay,z}$, $f_{moist,z}$ and $f_{temp,z}$ are functions depending respectively on the clay content, soil moisture and soil temperature at a given depth $z$, and range between 0 and 1.

The $f_{clay}$ function originated from the CENTURY model (Parton et al., 1987):

$$f_{clay,z} = 1 - 0.75 \times Clay_z \qquad (2)$$

where $Clay_z$ is the clay fraction (ranging between 0 and 1) of the soil at a given depth $z$.

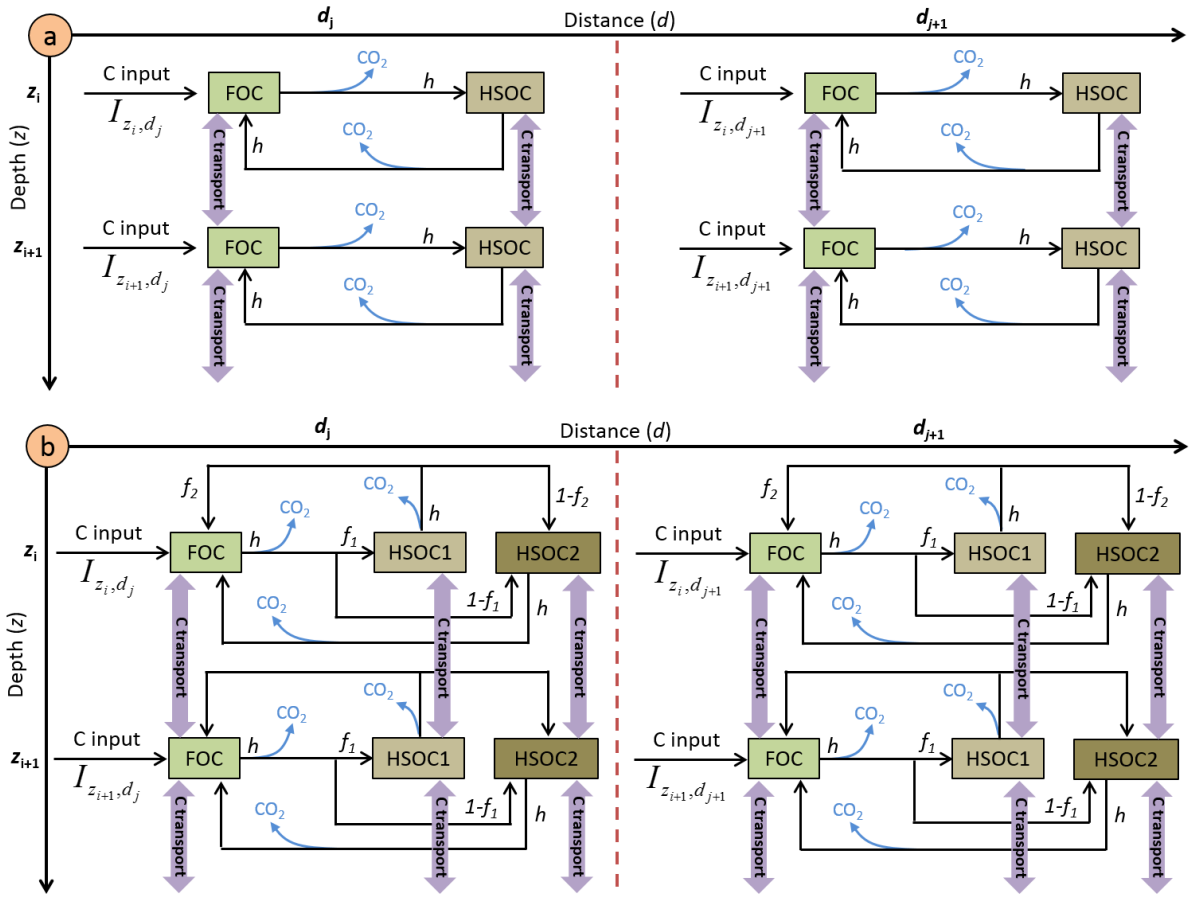


**Fig. 1.** Schematic representation of the pools and the fluxes of the (a) two pools model and (b) three pools model.

The $f_{moist,z}$ function originated from the meta-analysis of Moyano *et al.*, (2012) and is affected by soil properties (clay content, SOC content). Briefly, the authors fitted linear models on 310 soil incubations to describe the effect of soil moisture on decomposition. Then, they normalized such linear models between 0 and 1 to apply these functions to classical first order kinetics. All details are described in Moyano *et al.*, (2012). To save computing time, we calculated $f_{moist,z}$ only once using measured SOC stocks instead of using modelled SOC stocks and repeated the calculation at each time step.

The temperature sensitivity of the soil respiration is expressed as $Q_{10}$:

$$f_{temp,z} = Q_{10}^{\frac{temp_z - temp_{opt}}{10}} \quad (3)$$

with $temp_z$ being the soil temperature in K at each soil depth $z$ and $temp_{opt}$ a parameter fixed to 304.15 K. The $Q_{10}$ value was fixed to 2, a classical value used in models (Davidson and Janssens, 2006).

Once the FOC is decomposed, a fraction is humified ($h$) and another is respired as $CO_2$ ($1-h$) (Fig. 1a) following equations (4) and (5).

$$Humified\ FOC_{t,z,d} = h \times \frac{\partial FOC_{t,z,d}}{\partial t} \quad (4)$$

$$Respired\ FOC_{t,z,d} = (1-h) \times \frac{\partial FOC_{t,z,d}}{\partial t} \quad (5)$$

Two mathematical approaches are available in the model to describe the mineralisation of HSOC: a first order kinetics, as given by Eq. (6) or an approach developed by Wutzler & Reichstein, (2008) and by Guenet *et al.*, (2013) introducing the priming effect, i.e., the mineralisation of HSOC depends on FOC availability, and given by Eq. (7):

$$\frac{\partial HSOC_{t,z,d}}{\partial t} = -k_{HSOC,z} \times HSOC_{t,z,d} \times f_{moist,z} \times f_{temp,z} \quad (6)$$

$$\frac{\partial HSOC_{t,z,d}}{\partial t} = -k_{HSOC,z} \times HSOC_{t,z,d} \times (1 - e^{-PE \times FOC_{t,z,d}}) \times f_{moist,z} \times f_{temp,z} \quad (7)$$

where $HSOC_{t,z,d}$ is the humified SOC carbon pool at a given time ($t$, in years), depth ($z$, in m) and distance ($d$, in m), $k_{HSOC,z}$ is its decomposition rate ($yr^{-1}$) at a given depth $z$, and $PE$ is the priming effect parameter. The parameters $f_{moist,z}$ and $f_{temp,z}$ are functions depending respectively on soil moisture and soil temperature at a given depth $z$, and affecting the decomposition rate of HSOC. They correspond to the moisture equation from Moyano *et al.*, (2012) and to Eq. (3), respectively. The decomposition rate $k_{HSOC,z}$ was an exponential law depending on soil depth ($z$) as shown by an incubation study (see paragraph *HSOC decomposition rate* further in the M&M):

$$k_{HSOC,z} = a \times e^{-b \times z} \quad (8)$$

The $b$ parameter of this equation represented the ratio of labile C/stable C within the HSOC pool. The effect of clay on HSOC decomposition was implicitly taken into account in this equation as clay content increased with soil depth.

A fraction of decomposed HSOC returns to the FOC assuming that part of the HSOC decomposition products is as labile as FOC ($h$) and another is respired as $CO_2$ (Fig. 1a) in the two pools model.

Finally, we also developed an alternative version of the model with three pools by splitting the HSOC pools into two pools with different turnover rates, HSOC2 being more stabilized than HSOC1 (Fig. 1b). The non-respired decomposed FOC is split between HSOC1 and HSOC2 following a parameter $f_1$. The non-respired decomposed HSOC1 is split between HSOC2 and FOC following a parameter $f_2$ whereas non-respired decomposed HSOC2 is only redistributed into the FOC pools. The decomposition of HSOC1 and HSOC2 both follow the equation (8) but with different parameter values for $a$.

### 2.5.2 Carbon transport mechanisms

The transport of C between the different soil layers was represented by both advection and diffusion mechanisms (Elzein and Balesdent, 1995), which have been shown to usually describe well the C transport in soils (Bruun et al., 2007; Guenet et al., 2013). The advection represents the C transport due to the water infiltration in the soil, while the diffusion represents the C transport due to the fauna activity. The same transport coefficients were applied to the two C pools, FOC and HSOC.

The advection is defined by:

$$F_A = A \times C \qquad (9)$$

where $F_A$ is the flux of *C* transported downwards by advection, and *A* is the advection rate (mm $yr^{-1}$).

The diffusion is represented by the Fick's law:

$$F_D = -D \times \frac{\partial^2 C}{\partial z^2} \qquad (10)$$

where $F_D$ is the flux of C transported downwards by diffusion, $-D$ the diffusion coefficient ($cm^2$ $yr^{-1}$) and *C* the amount of carbon in the pool subject to transport (FOC or HSOC).

To represent the effect of soil tillage ($z \leq 0.2$ m), we added another diffusion term using the Fick's law but with a value of *D* several orders of magnitude higher to represent the mixing due to tillage. It must be noted that no tillage effect on the decomposition was represented here because of the large unknowns on these aspects (Dimassi et al., 2013; Virto et al., 2012).

In this model, the flux of *C* transported downwards by the advection and diffusion ($F_{AD}$) was represented as the sum of both mechanisms, following Elzein & Balesdent (1995):

$$F_{AD} = F_A + F_D \qquad (11)$$

The FOC and HSOC pools dynamics in the two pools model correspond to:

$$\frac{\partial FOC}{\partial t} = I_{t,z,d} + \frac{\partial F_{AD}}{\partial z} + h \times \frac{\partial HSOC_{t,z,d}}{\partial t} - \frac{\partial FOC_{t,z,d}}{\partial t} \qquad (12)$$

$$\frac{\partial HSOC}{\partial t} = \frac{\partial F_{AD}}{\partial z} + h \times \frac{\partial FOC_{t,z,d}}{\partial t} - \frac{\partial HSOC_{t,z,d}}{\partial t} \qquad (13)$$

Finally, the FOC, HSOC1 and HSOC2 pools dynamics in the three pools model correspond to:

$$\frac{\partial FOC}{\partial t} = I_{t,z,d} + \frac{\partial F_{AD}}{\partial z} + h \times f_2 \times \frac{\partial HSOC1_{t,z,d}}{\partial t} + h \times \frac{\partial HSOC2_{t,z,d}}{\partial t} - \frac{\partial FOC_{t,z,d}}{\partial t} \qquad (14)$$

$$\frac{\partial HSOC1}{\partial t\partial} = \frac{\partial F_{AD}}{\partial z} + h \times f_1 \times \frac{\partial FOC_{t,z,d}}{\partial t} - \frac{\partial HSOC1_{t,z,d}}{\partial t} \qquad (15)$$

$$\frac{\partial HSOC2}{\partial t} = \frac{\partial F_{AD}}{\partial z} + h \times (1 - f_1) \times \frac{\partial FOC_{t,z,d}}{\partial t} + h \times (1 - f_2) \times \frac{\partial HSOC1_{t,z,d}}{\partial t} - \frac{\partial HSOC2_{t,z,d}}{\partial t} \qquad (16)$$

### 2.5.3 Depth dependence of HSOC potential decomposition rates

The shape of the function (i.e. the *b* parameter) describing the HSOC potential decomposition rate (Eq. (8)) was determined by incubating soils from the control, the alley and the tree row, and from different soil layers (0.0-0.1, 0.1-0.3, 0.7-1.0 and 1.6-1.8 m). Soils were sieved at 5 mm, and incubated during 44 days at 20°C at a water potential of -0.03 MPa. Evolved $CO_2$ was measured using a micro-GC at 1, 3, 7, 14, 21, 28, 35, 44 days. The three first measurement dates corresponded to a pre-incubation period and were not included in the analysis. For a given depth, the cumulative mineralised SOC was expressed as a percentage of total SOC and was plotted against the incubation time. The slopes represented the potential SOC mineralisation rate at a given soil depth and location. The potential SOC mineralisation rates were then plotted

against soil depth (Fig. S1). We used the soil incubations to determine only the *b* parameter of the curve: with such short term incubations, the SOC decomposition rate over the soil profile is overestimated because the $CO_2$ measured during the incubations mainly originates from the labile C pool. The *a* parameter was optimized following the procedure described further.

### 2.6 Boundary conditions of the CARBOSAF model

#### 2.6.1 Annual aggregates of soil temperature and soil moisture

In April 2013, eight soil temperature and moisture sensors (Campbell CS 616 and Campbell 107, respectively) were installed in the agroforestry plot at 0.3, 1.3, 2.8 and 4.0 m depth, and at 2 and 5 m from the trees. Soil temperature and moisture were measured for 11 months.

The mean annual soil temperature in the agroforestry plot was described by the following equation:

$$T = -0.89 \times z + 288.24 \qquad (R^2 = 0.99) \qquad (17)$$

where $T$ is the soil temperature (K) and $z$ is the soil depth (m).

The mean annual soil moisture was described with the following equation:

$$\theta = 0.05 \times z + 0.28 \qquad (R^2 = 0.99) \qquad (18)$$

where $\theta$ is the soil volumetric moisture (cm $cm^{-3}$) and $z$ is the soil depth (m).

Due to a lack of data in the agricultural plot, we assumed that the soil temperature and the soil moisture were the same in the agroforestry tree rows, alleys and in the control plot, but we further performed a sensitivity analysis of the model on these two parameters.

#### 2.6.2 Interpolation of tree growth

The tree growth has been measured in the field since the establishment of the experiment. We used the diameter at breast height (*DBH*) as a surrogate of the tree growth preferentially to the

tree height as the field measurements were more accurate. Indeed, *DBH* is easier to measure than height, especially when trees are getting older. To describe the temporal dynamic of *DBH* since the tree planting, a linear equation was fitted on the data.

Tree growth measurements enabled us to fit the following equation that was used in the model:

$$DBH_t \begin{cases} 0.01, & t \leq 3 \\ 0.0157 \times t - 0.0391 \ (R^2 = 0.997) & 3 < t \leq 20 \end{cases} \quad (22\,19)$$

where $DBH_t$ is the diameter at breast height (m) and $t$ represents the time since tree planting (years).

### 2.6.3 Change of tree litterfall over time

For the five walnut trees where the leaf biomass was quantified, *DBH* was also measured. The ratio between the leaf biomass and *DBH* was then calculated for the five replicates. ~~A linear relationship between the leaf biomass and *DBH* was then considered to describe the increase of the leaf litter C input with the tree growth.~~ Total leaf biomass was 8.96 ± 1.45 kg DM tree$^{-1}$ and the carbon concentration of walnut leaves was 449.4 ± 3.7 mg C g$^{-1}$ (Table 2). With a density of 110 trees ha$^{-1}$, leaf litterfall was estimated at 0.73 ± 0.06 t C ha$^{-1}$ in 2012 and at the plot scale. The ratio between leaf biomass and *DBH* was 0.0277 ± 0.0024 t C tree$^{-1}$ m$^{-1}$ or 3.05 t C ha$^{-1}$ m$^{-1}$. The following linear relationship was therefore used in the model to describe leaf litter C input with the tree growth:

$$L_t = 3.05 \times DBH_t \quad (2\,60)$$

where $L_t$ is the leaf litter input (t C ha$^{-1}$) at the year $t$, and $DBH_t$ the diameter at breast height (m) the year $t$.

### 2.6.4 Tree fine root C input from mortality

In 2012, the measured tree fine root biomass was higher in the tree row than in the alley (Table S1). From 0 to 1 m distance from the tree (in the tree row), the tree fine root biomass was homogeneous and was 1.01 t C $ha^{-1}$ down 2 m depth.

~~A decreasing exponential function was fitted on the root biomass data obtained from the pit in 2012 to describe total fine root biomass (*TFRB*) down to 2 m depth as a function of distance from the tree.~~ In 2012 and in the alley, the tree fine root biomass (*TFRB*) decreased with increasing distance from the tree and was represented by an exponential function:

$$TFRB = \begin{cases} 1.01, & 0 \le d \le 1 \\ 1.29 \times e^{-0.28 \times d} \quad (R^2 = 0.90), & 1 < d \le 6.5 \end{cases} \qquad (2~~7~~1)$$

where *TFRB* represents tree fine root biomass down 2 m depth (t C $ha^{-1}$), and *d* the distance from the tree (m).

We considered a linear increase of *TFRB* with increasing *DBH*, and a linear regression was performed between *TFRB* in 2012 and *TFRB* in 1996, the first year after planting (biomass considered as negligible). The following linear relationship was used to simulate *TFRB* as a function of tree growth:

$$TFRB_{t,d} = \begin{cases} 3.69 \times DBH_t, & 0 \le d \le 1 \\ 4.70 \times DBH_t \times e^{-0.28 \times d}, & 1 < d \le 6.5 \end{cases} \qquad (2~~8~~2)$$

where $TFRB_t$ represents the tree fine root biomass to 2 m depth (t C $ha^{-1}$) at the year *t*, $DBH_t$ the diameter at breast height (m) at the year *t*, and *d* the distance to the tree (m).

A changing distribution of tree fine roots within the soil profile was taken into account with increasing distance to the tree. For this purpose, exponential functions ($a \times e^{-b \times z}$) were fitted in the alley every 0.5 m distance, and a linear regression was fitted between their coefficients *a* and *b* and distance from the tree. However, the distribution of *TFRB* within the soil profile and with the distance to the tree was considered constant with time.

A decreasing exponential function best represented the changing distribution of tree fine roots within the soil profile with increasing distance to the tree:

$$p_{TFRB,z,d} = \begin{cases} 13.92 \times e^{-1.39 \times z} \quad (R^2 = 0.68), & 0 \le d \le 1 \\ a \times e^{-b \times z}, & 1 < d \le 6.5 \end{cases} \quad (2\text{~~3~~}3)$$

and

$$a = 10.31 - 1.15 \times d \quad (R^2 = 0.69) \quad (\text{~~30~~}24)$$

$$b = -1.10 + 0.19 \times d \quad (R^2 = 0.51) \quad (\text{~~31~~}25)$$

Finally,

$$p_{TFRB,z,d} = \begin{cases} 13.92 \times e^{-1.39 \times z}, & 0 \le d \le 1 \\ (10.31 - 1.15 \times d) \times e^{-(-1.10+0.19 \times d) \times z}, & 1 < d \le 6.5 \end{cases} \quad (\text{~~3~~}26)$$

where $p_{TFRB,z,d}$ is the proportion (%) of the total tree fine root biomass (*TFRB*) at a given depth *z* (m), and at a distance *d* from the tree (m).

To finally estimate the tree fine root input due to the mortality, *TFRB* was multiplied by the measured root turnover. The tree fine root turnover ranged from 1.7 to 2.8 $yr^{-1}$ depending on fine root diameter, with an average turnover of 2.2 $yr^{-1}$ for fine roots ≤ 2 mm and to a depth of 2 m (Germon et al., 2016).

### 2.6.5 Aboveground and belowground input from the crop

As there were more crop yield measurements (14) than straw biomass measurements (6), the effect of agroforestry on the crop yield with time was used as an estimate for change in the aboveground and belowground wheat biomass.

For this, the relative yield ($Rel\ Y_{AF}$) in the agroforestry system was calculated for each year as the ratio between the agroforestry yield and the control yield ($Y_C$). ~~A linear regression was then fitted between the relative yield and the *DBH*.~~

The average annual crop yield in the control plot was $Y_C$ = 3.79 ± 0.40 t DM ha$^{-1}$ for the 14 studied years. In the agroforestry plot, the average relative yield decreased linearly with time (increasing *DBH*) and was described using the following linear equation (Fig. 2):

$$Rel\ Y_{AF_t} = -93.33 \times DBH_t + 100 \qquad (R^2 = 0.12, \qquad p - value = 0.02) \qquad (27)$$

where $Rel\ Y_{AF_t}$ is the average relative crop yield (%) in the agroforestry plot compared to the control plot at year *t*, and $DBH_t$ is the diameter at breast height (m) at year *t*.

The variation of crop yield with distance from the trees was described with a quadratic equation (Fig. 2). But as we aimed to predict SOC stocks up to 6.5 m distance from the trees (middle of the alley), a linear increase of crop yield with increasing distance from the tree gave similar results as the quadratic equation over the 6.5 m distance and was more parsimonious.

~~: In the agroforestry plot, a linear relationship was used to describe the relative crop yield increase from the tree to the middle of the alley (Fig. 2):~~

$$Rel\ Y_{AF_d} = 4.39 \times d + 64.57 \quad (R^2 = 0.24), \qquad 1 < d \leq 6.5 \qquad (28)$$

where $Rel\ Y_{AF_d}$ is the relative crop yield (%) in the agroforestry plot at a distance *d* (m) from the tree compared to the control plot.

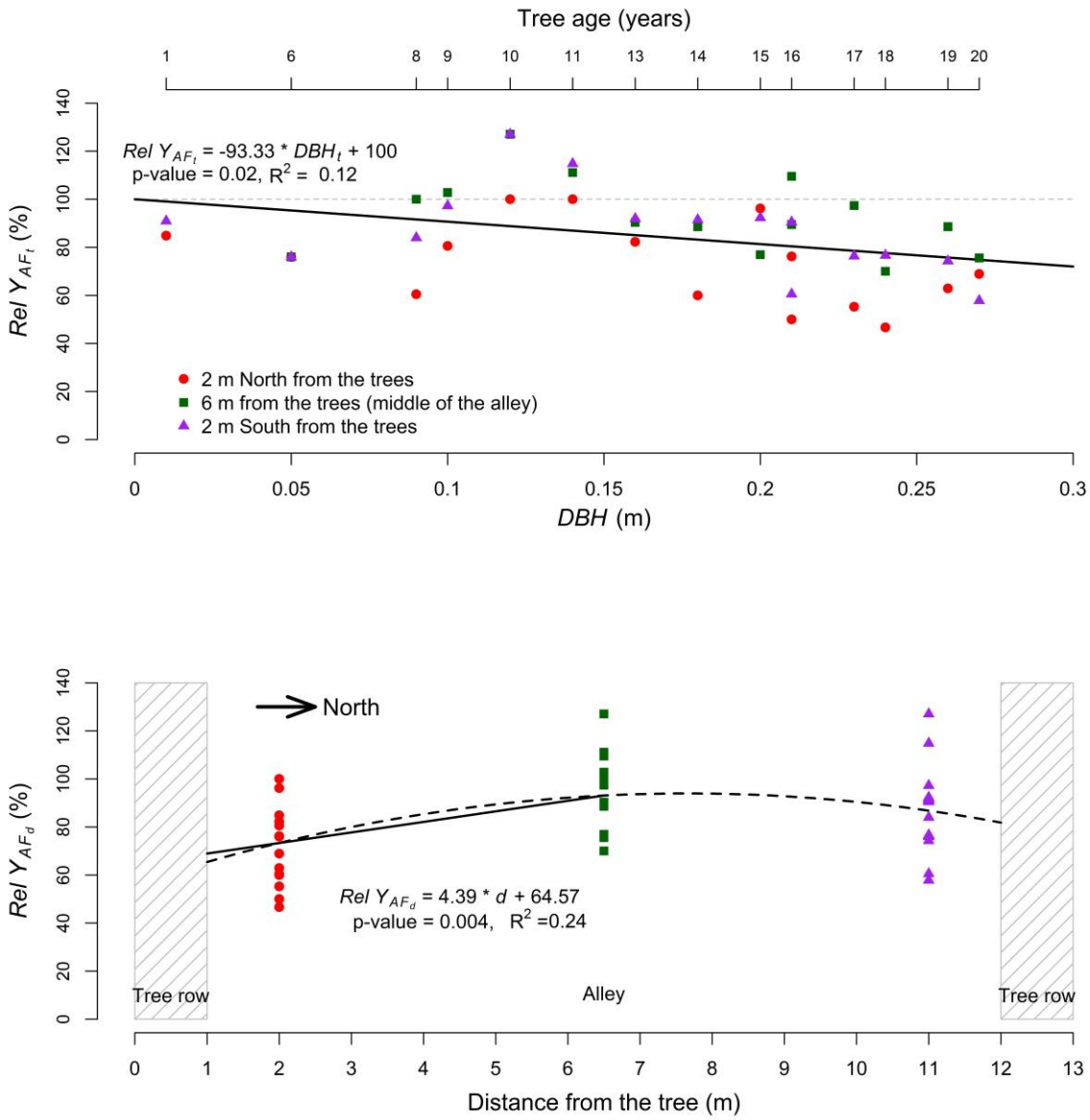


**Fig. 2.** Top: Relative yield ($Rel\ Y_{AF_t}$) in the agroforestry plot compared to the control plot as a function of tree growth, represented by the diameter at breast height (*DBH*) at year *t*. Bottom: Relative yield ($Y_{AF_{t,d}}$) as a function of the distance from the tree.

Finally, the crop yield in the agroforestry plot was modeled as follows:

$$Y_{AF_{t,d}} = Rel\ Y_{AF_t} \times Y_C \times Rel\ Y_{AF_d} \quad (R^2 = 0.19), \quad 1 < d \leq 6.5 \quad (2\sout{9}5)$$

where $Y_{AF_{t,d}}$ is the crop yield (t DM ha$^{-1}$) in the agroforestry plot at the year *t* and at a distance *d* (m) from the tree. Because three linear equations were used to describe the crop yield in the agroforestry plot, errors were accumulated and we finally came up with a standard underestimation of the crop yield in the agroforestry plot that we corrected by multiplying our equation by 1.2.

~~Finally, t~~The ratio between the straw biomass and the crop yield was calculated as the average of the six measurements, and was considered constant with time. This ratio was used to convert crop yield into straw biomass. In the agroforestry plot, the carbon input to the soil from the aboveground crop biomass was:

$$ABC_{crop,t,d} = Y_{AF_{t,d}} \times (straw\ biomass{:}\ crop\ yield) \times C_{straw} \times (1 - export) \quad (3~~0~~)$$

where $ABC_{crop,t,d}$ is the aboveground carbon input from the crop (t C ha$^{-1}$) at the year *t* and distance *d* from the tree, $Y_{AF_{t,d}}$ is the agroforestry crop yield. The average ratio between the straw biomass (t DM ha$^{-1}$) and the crop yield (t DM ha$^{-1}$) equaled 1.03 ± 0.11 (n=6). The wheat straw was exported out of the field after the harvest, but it was estimated that 25% of the straw biomass was left on the soil, thus *export*=0.75. In the control plot, $Y_{AF_{t,d}}$ was replaced by $Y_C$.

To estimate fine root biomass of the crop, we hypothesized that the root:shoot ratio of the durum wheat was the same in both the agroforestry and agricultural plot, in the absence of any published data on the matter. In the agroforestry plot, the belowground crop biomass was represented by:

$$BEC_{crop,t,d} = Y_{AF_{t,d}} \times (shoot{:}\ crop\ yield) \times (root{:}\ shoot) \times C_{root} \quad (31)$$

where $BEC_{crop,t,d}$ is the belowground crop biomass (t C ha$^{-1}$) at the year *t* and at a distance *d* from the tree, $Y_{AF_{t,d}}$ is the agroforestry crop yield. The average ratio between the total crop

aboveground biomass (*shoot*) and the crop yield equaled 2.45 ± 0.15 (n=6). In 2012, total fine root biomass was 2.29 ± 0.32 t C $ha^{-1}$ in the control (Table 3).

**Table 3.** Wheat fine root biomass in the agricultural control plot in 2012.

| Soil depth (m) | Wheat fine root biomass (kg C $m^{-3}$) | (t C $ha^{-1}$) |
|---|---|---|
| 0.0-0.1 | 0.48 ± 0.05 | 0.48 ± 0.05 |
| 0.1-0.3 | 0.34 ± 0.04 | 0.69 ± 0.09 |
| 0.3-0.5 | 0.22 ± 0.04 | 0.44 ± 0.08 |
| 0.5-1.0 | 0.10 ± 0.04 | 0.52 ± 0.20 |
| 1.0-1.5 | 0.03 ± 0.04 | 0.17 ± 0.19 |
| Total | - | 2.29 ± 0.32 |

Errors represent standard errors.

Therefore, the wheat *root:shoot* ratio equaled 0.79 ± 0.12 (n=1). The carbon concentration of wheat root was $C_{root}$ = 35.14 ± 1.90 mg C $g^{-1}$. In the control plot, $Y_{AF_{t,d}}$ was replaced by $Y_C$.

In 2012, no wheat roots were observed below 1.5 m, and root biomass decreased exponentially with increasing depth (Table 3). The distribution of crop roots within the soil profile was described as follows:

$$p_{CRBc,z} = \begin{cases} 26.44 \times e^{-2.59 \times z} & (R^2 = 0.99), \quad z \leq 1.5 \\ 0, & z > 1.5 \end{cases} \qquad (32)$$

where $p_{CRBc,z}$ is the proportion (%) of total crop root biomass in the control plot at a given depth z (m).

Since the same maximum rooting depth of the crop was observed in the agroforestry plot and in the control plot, we inferred that the wheat root distribution within the soil profile was not modified by agroforestry, but only its biomass. The crop root turnover was assumed to be 1 $yr^{-1}$, root mortality occurring mainly after crop harvest.

~~The wheat root distribution within the soil profile as a function of total wheat root biomass was described by an exponential fit. Since the same maximum rooting depth of the crop was observed in the agroforestry plot and in the control plot, we inferred that the wheat root distribution within the soil profile was not modified by agroforestry, but only its biomass.~~

### 2.6.6 Aboveground and belowground input from herbaceous vegetation in the tree rows

~~We fitted an exponential function to describe the herbaceous root biomass with depth. We assumed for simplification that the aboveground and belowground biomasses of the herbaceous vegetation in the tree row were constant over time.~~The distance from the trees had no effect on the above and belowground biomass of the herbaceous vegetation (data not shown), therefore average values are presented. The summer aboveground biomass was almost three times higher than in winter, whereas the belowground biomass was two times higher (Table 4). The total aboveground carbon input was 2.13 ± 0.14 t C $ha^{-1}$ $yr^{-1}$ and the total belowground carbon input was 0.74 ± 0.05 t C $ha^{-1}$ $yr^{-1}$ to 0.5 m depth.

**Table 4.** Aboveground and belowground biomass of the herbaceous vegetation in the tree rows.

| | | Herbaceous biomass (t C $ha^{-1}$) | |
|---|---|---|---|
| | Soil depth (m) | Summer | Winter |
| Aboveground | - | 1.57 ± 0.11 | 0.56 ± 0.09 |
| Belowground | 0.0-0.1 | 0.22 ± 0.03 | 0.17 ± 0.01 |
| | 0.1-0.3 | 0.16 ± 0.02 | 0.06 ± 0.01 |
| | 0.3-0.5 | 0.09 ± 0.04 | 0.04 ± 0.01 |
| | Total | 0.46 ± 0.04 | 0.27 ± 0.02 |

Errors represent standard errors.

The belowground carbon input from the tree row vegetation ($BEC_{veg,z}$, t C $ha^{-1}$) at a given depth z (m) was described by the following equation:

$$BEC_{veg,z} = \begin{cases} 0.44 \times e^{-3.12 \times z}, & z \leq 1.5 \\ 0, & z > 1.5 \end{cases} \quad (33)$$

We assumed for simplification that the aboveground and belowground biomasses of the herbaceous vegetation in the tree row were constant over time.

### 2.7 Optimization procedure

Depending on the model variant, four to ~~F~~five parameters were optimized with a Bayesian statistical method (Santaren et al., 2007; Tarantola, 1987, 2005) using measured SOC stocks from the control plot only. These parameters were *A*, the advection rate, *D*, the diffusion coefficient, *h* the humification yield, *a* the coefficient of the $k_{HSOC}$ rate from Eq. (10), and *PE* the priming coefficient. These four or five parameters were calibrated so that equilibrium SOC stocks, i.e. after 5000 years of simulation, equaled SOC stocks of the control plot in 2013. ~~SOC pools were initialized after a spin-up of 5000 years in the control plot. Measured SOC stocks in 2013 in the control plot were used for the spin-up.~~ The associated uncertainty was estimated with the 93 soil cores sampled in the control plot (see section 2.2.1). Due to a lack of relevant data, we assumed that the climate and the land use were the same for the last 5000 years, and that SOC stocks in the control plot were at equilibrium at the time of measurement. Therefore, SOC stocks at the end of the ~~spin-up~~5000 years of simulation equaled SOC stocks in the control plot. Three different ~~spin-ups~~calibrations were performed, corresponding to the three different models that were used: one ~~spin-up~~calibration with the two pools model without the priming effect, one ~~spin-up~~calibration with the two pools model with the priming effect, and one ~~spin-up~~calibration with the three pools model.

~~The~~ Each model variant was fitted to the control SOC stocks data using a Bayesian curve fitting method described in Tarantola (1987), after a conversion from SOC stocks in kg C $m^{-2}$ to SOC stocks in kg $m^{-3}$ due to the different soil layers' thickness. We aimed to find a parameter set that minimizes the distance between model outputs and the corresponding observations, considering model and data uncertainties, and prior information on parameters. With the

assumption of Gaussian errors for both the observations and the prior parameters, the optimal parameter set corresponds to the minimum of the cost function $\boldsymbol{J}(\boldsymbol{x})$:

$$\boldsymbol{J}(\boldsymbol{x}) = 0.5 \times \left[(\boldsymbol{y} - \boldsymbol{H}(\boldsymbol{x}))^t \times \boldsymbol{R}^{-1} \times \left(\boldsymbol{y} - \boldsymbol{H}(\boldsymbol{x})\right) + (\boldsymbol{x} - \boldsymbol{x}_b)^t \times {\boldsymbol{P}_b}^{-1} \times (\boldsymbol{x} - \boldsymbol{x}_b)\right] \quad (\text{~~19~~}34)$$

that contains both the mismatch between modelled and observed SOC stock and the mismatch between a priori and optimized parameters. $\boldsymbol{x}$ is the vector of unknown parameters, $\boldsymbol{x}_b$ the vector of a priori parameter values, $\boldsymbol{H()}$ the model and $y$ the vector of observations. The covariance matrices $\boldsymbol{P}_b$ and $\boldsymbol{R}$ describe a priori uncertainties on parameters, and observations, respectively. Both matrices are diagonal as we suppose the observation uncertainties and the parameter uncertainties to be independent. To determine an optimal set of parameters which minimizes $\boldsymbol{J}(\boldsymbol{x})$, we used the B~~G~~FGS gradient-based algorithm (Tarantola, 1987). ~~We~~ For each model variant, we performed 30 optimizations starting with different parameter prior values to check that the results did not correspond to a local minimum. ~~To optimize the parameters we only used the data coming from the control plot.~~ As the BFGS algorithm does not directly calculate the variance of posteriors, they were quantified using the curvature cost function at its minimum once it was reached (Santaren et al., 2007).

### 2.8 Comparison of models

Model predictions with and without priming effect were compared calculating the coefficients of determination, root mean square errors (RMSE) and Bayesian information criteria (BIC).

$$RMSE = \sqrt{\frac{1}{N}\sum_{i=1}^{N}(x_i - \bar{x})^2} \qquad (\text{~~20~~}35)$$

where $i$ is the number of observations (1 to N), $x_i$ is the predicted value and $\bar{x}$ is the mean observed value.

$$BIC = N \times \ln(MSD) + k \times \ln(N) \qquad (\text{~~21~~}36)$$

where *N* is the number of observations, *MSD* is the mean squared deviation used to estimate the maximum likelihood (Manzoni et al., 2012), and *k* is the number of model parameters.

The model was run at a yearly time step using mean annual soil temperature and moisture and annual C inputs to the soil. ~~SOC pools were initialized after a spin-up of 5000 years in the control plot. Measured SOC stocks in 2013 in the control plot were used for the spin-up. The associated uncertainty was estimated with the 93 soil cores sampled in the control plot (see section 2.2.1). Due to a lack of relevant data, we assumed that the climate and the land use were the same for the last 5000 years, and that SOC stocks in the control plot were at equilibrium. Therefore, SOC stocks at the end of the spin-up equaled SOC stocks in the control plot. Three different spin-ups were performed, corresponding to the three different models that were used: one spin-up with the two pools model without the priming effect, one spin-up with the two pools model with the priming effect, and one spin-up with the three pools model.~~ In the agroforestry, the model was run from the ground (0 m) to 2 m depth, and from the tree (0 m) to 6.5 m from the tree (middle of the alley). The model was applied separately across locations of a tree-distance gradient having varying OC inputs, each soil column was considered independent from another. SOC pools were initialized after a spin-up of 5000 years in the control plot. At $t_0$, SOC stocks in the agroforestry plot therefore equaled SOC stocks of the control plot. The model was then run from $t_0$ to $t_{18}$ (years) after tree planting. The spatial resolution was 0.1 m both vertically and horizontally. The model was developed using R 3.1.1 (R Development Core Team, 2013). Partial-differential equations were solved using the R package *deSolve* and the *ode.1D* method (Soetaert et al., 2010).

**2.9 Estimation of the priming intensity and its impact on SOC storage**

In equation (7), the priming effect (*PE*) is considered as a control of the FOC on the HSOC decomposition and not as an accelerating factor of the HSOC decomposition. This method followed the Wutzler & Reichstein, (2008) approach based on the microbial biomass and adapted to the FOC by Guenet *et al.*, (2013) for models without explicit microbial biomass. Models able to reproduce priming effect generally need an explicit microbial biomass controlling the decomposition (Blagodatsky et al., 2010; Perveen et al., 2014). The priming scheme used here allows some simplifications in the model structure since an explicit representation of the microbial biomass is not needed. Furthermore, at equilibrium state (i.e. when the input rate is constant) the decomposition rate of a first order equation (Eq. (6)) takes *PE* implicitly into account. Indeed, when FOC enters the system, there is an induced priming, a constant FOC input rate therefore induces a constant priming. This means that when we optimized the decomposition rate parameter in the control plot, we implicitly represented this priming but at a fixed rate. When FOC inputs are modified, due to the tree growth for instance, the *PE* intensity is modified and this effect cannot be represented by classical first order kinetics. To estimate the importance of priming on SOC storage in the agroforestry plot, the simulations using first order equations (Eq. (6)) can therefore not be directly compared to the simulations using the FOC-dependant decomposition rate (Eq. (7)). To estimate the change of SOC decomposition rate due to priming when trees are planted, the decomposition ~~rate~~ fluxes predicted by Eq. (7) $\left(-k_{HSOC,z} \times (1 - e^{-PE \times FOC_{t,z,d}})\right)$ in the agroforestry plot ~~has to~~ must be compared to the fluxes in the agroforestry plot using the decomposition rate from the control plot calculated by Eq. (7) with $FOC_{t,z,d}$ corresponding to the FOC inputs in the control plot.~~decomposition rate.~~ Thus, to calculate the importance of priming on SOC storage when trees are planted, we used the decomposition rates calculated following Eq. (7) in the control plot $\left(-k_{HSOC,z} \times (1 - e^{-PE \times FOC_{t,z,d}})\right)$ and we applied this decomposition rate to the agroforestry plot as a classical first order kinetics (without the control FOC ~~from the control~~

plot, i.e. $k_{new} = -k_{HSOC,z} \times (1 - e^{-PE \times FOC_{t,z,d}})$ with $FOC_{t,z,d}$ fixed constant). This simulation corresponded to the absence of priming due to trees in the agroforestry plot (i.e. decomposition not controlled by the FOC of the agroforestry plot). By difference with the simulation performed with the full two pools model (Eq. (7)), i.e., taking account of FOC input and priming, we calculated the priming intensity.

## 3 Results

### 3.1 Experimental results

#### 3.1.1 Carbon stock in the walnut tree biomass

The measured aboveground (trunk + branches) and stump carbon stock of 18-year-old walnut trees are presented in Table 3.

**Table 3.** Carbon stocks in the aboveground biomass and in the stump of 18-year-old walnut trees (110 trees ha$^{-1}$).

| | Tree biomass carbon stock | |
|---|---|---|
| | (kg C tree$^{-1}$) | (t C ha$^{-1}$) |
| Trunk | 55.06 ± 4.35 | 6.06 ± 0.48 |
| Branches | 40.98 ± 7.65 | 4.51 ± 0.84 |
| Stump | 21.21 ± 1.07 | 2.33 ± 0.12 |
| Total | 117.25 ± 8.87 | 12.9 ± 0.98 |

Errors represent standard errors.

#### 3.1.2 Tree growth

Tree growth measurements enabled us to fit the following equation that was used in the model:

$$DBH_t \begin{cases} 0.01, & t \leq 3 \\ 0.0157 \times t - 0.0391 \ (R^2 = 0.997) & 3 < t \leq 20 \end{cases} \quad (22)$$

where $DBH_t$ is the diameter at breast height (m) and $t$ represents the time since tree planting (years).

### 3.1.3 Crop yield

The average annual crop yield in the control plot was $Y_C = 3.79 \pm 0.40$ t DM ha$^{-1}$ for the 14 studied years. In the agroforestry plot, the average relative yield decreased linearly with time (increasing *DBH*) and was described using the following linear equation (Fig. 2):

$$Rel\ Y_{AF_t} = -93.33 \times DBH_t + 100 \qquad (R^2 = 0.12, \qquad p - value = 0.02) \qquad (23)$$

where $Rel\ Y_{AF_t}$ is the average relative crop yield (%) in the agroforestry plot compared to the control plot at year *t*, and $DBH_t$ is the diameter at breast height (m) at year *t*.

In the agroforestry plot, a linear relationship was used to describe the relative crop yield increase from the tree to the middle of the alley (Fig. 2):

$$Rel\ Y_{AF_d} = 4.39 \times d + 64.57 \quad (R^2 = 0.24), \qquad 1 < d \leq 6.5 \qquad (24)$$

where $Rel\ Y_{AF_d}$ is the relative crop yield (%) in the agroforestry plot at a distance *d* (m) from the tree compared to the control plot.

Finally, the crop yield in the agroforestry plot was modeled as follows:

$$Y_{AF_{t,d}} = Rel\ Y_{AF_t} \times Y_C \times Rel\ Y_{AF_d} \quad (R^2 = 0.19), \qquad 1 < d \leq 6.5 \qquad (25)$$

where $Y_{AF_{t,d}}$ is the crop yield (t DM ha$^{-1}$) in the agroforestry plot at the year *t* and at a distance *d* (m) from the tree. Because three linear equations were used to describe the crop yield in the agroforestry plot, errors were accumulated and we finally came up with a standard underestimation of the crop yield in the agroforestry plot that we corrected by multiplying our equation by 1.2.

**Fig. 2.** Top: Relative yield ($Rel\ Y_{AF_t}$) in the agroforestry plot compared to the control plot as a function of tree growth, represented by the diameter at breast height (*DBH*) at year *t*. Bottom: Relative yield ($Y_{AF_{t,d}}$) as a function of the distance from the tree.

### 3.2 Carbon inputs to the FOC pool

#### 3.2.1 Leaf litterfall

Total leaf biomass was 8.96 ± 1.45 kg DM tree$^{-1}$ and the carbon concentration of walnut leaves was 449.4 ± 3.7 mg C g$^{-1}$ (Table 2). With a density of 110 trees ha$^{-1}$, leaf litterfall was estimated at 0.73 ± 0.06 t C ha$^{-1}$ in 2012 and at the plot scale. The ratio between leaf biomass and *DBH* was 0.0277 ± 0.0024 t C tree$^{-1}$ m$^{-1}$ or 3.05 t C ha$^{-1}$ m$^{-1}$. The following linear relationship was therefore used in the model to describe leaf litter C input:

$$L_t = 3.05 \times DBH_t \qquad (26)$$

where $L_t$ is the leaf litter input (t C ha$^{-1}$) at the year *t*, and $DBH_t$ the diameter at breast height (m) the year *t*.

#### 3.2.2 Tree fine root C input from mortality

In 2012, the measured tree fine root biomass was higher in the tree row than in the alley (Table 4). From 0 to 1 m distance from the tree (in the tree row), the tree fine root biomass was homogeneous and was 1.01 t C ha$^{-1}$ down 2 m depth.

**Table 4.** Walnut tree fine root biomass (t C ha$^{-1}$) as a function of depth and distance from the trees (m).

| | Tree fine root biomass (t C ha$^{-1}$) | | | |
|---|---|---|---|---|
| | Tree row | | Alley | |
| Soil depth (m) | [0, 1] m | ]1, 2.5] m | ]2.5, 4.0] m | ]4.0, 5.5] m |
| 0.0–0.1 | 0.08 ± 0.01 | 0.08 ± 0.01 | 0.01 ± 0.00 | 0.00 ± 0.00 |
| 0.1–0.3 | 0.14 ± 0.02 | 0.24 ± 0.02 | 0.15 ± 0.02 | 0.05 ± 0.01 |

| | | | | |
|---|---|---|---|---|
| 0.3-0.5 | 0.22 ± 0.02 | 0.16 ± 0.02 | 0.08 ± 0.01 | 0.05 ± 0.01 |
| 0.5-1.0 | 0.35 ± 0.04 | 0.14 ± 0.01 | 0.14 ± 0.01 | 0.08 ± 0.01 |
| 1.0-1.5 | 0.15 ± 0.02 | 0.10 ± 0.01 | 0.08 ± 0.01 | 0.08 ± 0.01 |
| 1.5-2.0 | 0.07 ± 0.01 | 0.13 ± 0.01 | 0.09 ± 0.01 | 0.07 ± 0.01 |
| Total | 1.01 ± 0.06 | 0.84 ± 0.04 | 0.55 ± 0.03 | 0.34 ± 0.02 |

Data modified from . Errors represent standard errors.

In 2012 and in the alley, the tree fine root biomass decreased with increasing distance from the tree and was represented by an exponential function:

$$TFRB = \begin{cases} 1.01, & 0 \le d \le 1 \\ 1.29 \times e^{-0.28 \times d} \quad (R^2 = 0.90), & 1 < d \le 6.5 \end{cases} \qquad (27)$$

where *TFRB* represents tree fine root biomass down 2 m depth (t C ha$^{-1}$), and *d* the distance from the tree (m).

The following linear relationship was used to simulate *TFRB* as a function of tree growth:

$$TFRB_{t,d} = \begin{cases} 3.69 \times DBH_t, & 0 \le d \le 1 \\ 4.70 \times DBH_t \times e^{-0.28 \times d}, & 1 < d \le 6.5 \end{cases} \qquad (28)$$

where $TFRB_t$ represents the tree fine root biomass to 2 m depth (t C ha$^{-1}$) at the year *t*, $DBH_t$ the diameter at breast height (m) at the year *t*, and *d* the distance to the tree (m).

A decreasing exponential function best represented the changing distribution of tree fine roots within the soil profile with increasing distance to the tree:

$$p_{TFRB,z,d} = \begin{cases} 13.92 \times e^{-1.39 \times z} \quad (R^2 = 0.68), & 0 \le d \le 1 \\ a \times e^{-b \times z}, & 1 < d \le 6.5 \end{cases} \qquad (29)$$

and

$$a = 10.31 - 1.15 \times d \quad (R^2 = 0.69) \qquad (30)$$

$$b = -1.10 + 0.19 \times d \quad (R^2 = 0.51) \qquad (31)$$

Finally,

$$p_{TFRB,z,d} = \begin{cases} 13.92 \times e^{-1.39 \times z}, & 0 \le d \le 1 \\ (10.31 - 1.15 \times d) \times e^{-(-1.10+0.19 \times d) \times z}, & 1 < d \le 6.5 \end{cases} \quad (32)$$

where $p_{TFRB,z,d}$ is the proportion (%) of the total tree fine root biomass (*TFRB*) at a given depth *z* (m), and at a distance *d* from the tree (m).

The tree fine root turnover ranged from 1.7 to 2.8 $yr^{-1}$ depending on fine root diameter, with an average turnover of 2.2 $yr^{-1}$ for fine roots ≤ 2 mm and to a depth of 2 m (Germon et al., 2016).

### 3.2.3 Aboveground carbon input from the crop

In the agroforestry plot, the carbon input to the soil from the aboveground crop biomass was:

$$ABC_{crop,t,d} = Y_{AF_{t,d}} \times (straw\ biomass{:}\ crop\ yield) \times C_{straw} \times (1 - export) \quad (33)$$

where $ABC_{crop,t,d}$ is the aboveground carbon input from the crop (t C $ha^{-1}$) at the year *t* and distance *d* from the tree, $Y_{AF_{t,d}}$ is the agroforestry crop yield. The average ratio between the straw biomass (t DM $ha^{-1}$) and the crop yield (t DM $ha^{-1}$) equaled 1.03 ± 0.11 (n=6). The wheat straw was exported out of the field after the harvest, but it was estimated that 25% of the straw biomass was left on the soil, thus *export*=0.75. In the control plot, $Y_{AF_{t,d}}$ was replaced by $Y_C$.

### 3.2.4 Belowground carbon input from the crop

In the agroforestry plot, the belowground crop biomass was represented by:

$$BEC_{crop,t,d} = Y_{AF_{t,d}} \times (shoot{:}\ crop\ yield) \times (root{:}\ shoot) \times C_{root} \quad (34)$$

where $BEC_{crop,t,d}$ is the belowground crop biomass (t C $ha^{-1}$) at the year *t* and at a distance *d* from the tree, $Y_{AF_{t,d}}$ is the agroforestry crop yield. The average ratio between the total crop aboveground biomass (*shoot*) and the crop yield equaled 2.45 ± 0.15 (n=6). In 2012, total fine root biomass was 2.29 ± 0.32 t C $ha^{-1}$ in the control (Table 5).

**Table 5.** Wheat fine root biomass in the agricultural control plot in 2012.

| Soil depth (m) | Wheat fine root biomass ($kg\ C\ m^{-3}$) | ($t\ C\ ha^{-1}$) |
|---|---|---|
| 0.0–0.1 | 0.48 ± 0.05 | 0.48 ± 0.05 |
| 0.1–0.3 | 0.34 ± 0.04 | 0.69 ± 0.09 |
| 0.3–0.5 | 0.22 ± 0.04 | 0.44 ± 0.08 |
| 0.5–1.0 | 0.10 ± 0.04 | 0.52 ± 0.20 |
| 1.0–1.5 | 0.03 ± 0.04 | 0.17 ± 0.19 |
| Total | - | 2.29 ± 0.32 |

Errors represent standard errors.

Therefore, the wheat *root:shoot* ratio equaled 0.79 ± 0.12 (n=1). The carbon concentration of wheat root was $C_{root}$ = 35.14 ± 1.90 mg C $g^{-1}$. In the control plot, $Y_{AF_{t,d}}$ was replaced by $Y_C$.

In 2012, no wheat roots were observed below 1.5 m, and root biomass decreased exponentially with increasing depth (Table 5). The distribution of crop roots within the soil profile was described as follows:

$$p_{CRBc,z} = \begin{cases} 26.44 \times e^{-2.59 \times z} & (R^2 = 0.99), \quad z \leq 1.5 \\ 0, & z > 1.5 \end{cases} \quad (35)$$

where $p_{CRBc,z}$ is the proportion (%) of total crop root biomass in the control plot at a given depth $z$ (m).

The crop root turnover was assumed to be 1 $yr^{-1}$, root mortality occurring mainly after crop harvest.

### 3.2.5 Aboveground and belowground carbon inputs from the tree row herbaceous vegetation

The distance from the trees had no effect on the above and belowground biomass of the herbaceous vegetation (data not shown), therefore average values are presented. The summer aboveground biomass was almost three times higher than in winter, whereas the belowground

biomass was two times higher (Table 6). The total aboveground carbon input was 2.13 ± 0.14 t C $ha^{-1}$ $yr^{-1}$ and the total belowground carbon input was 0.74 ± 0.05 t C $ha^{-1}$ $yr^{-1}$ to 0.5 m depth.

**Table 6.** Aboveground and belowground biomass of the herbaceous vegetation in the tree rows.

| | | Herbaceous biomass (t C $ha^{-1}$) | |
|---|---|---|---|
| | Soil depth (m) | Summer | Winter |
| Aboveground | - | 1.57 ± 0.11 | 0.56 ± 0.09 |
| Belowground | 0.0–0.1 | 0.22 ± 0.03 | 0.17 ± 0.01 |
| | 0.1–0.3 | 0.16 ± 0.02 | 0.06 ± 0.01 |
| | 0.3–0.5 | 0.09 ± 0.04 | 0.04 ± 0.01 |
| | Total | 0.46 ± 0.04 | 0.27 ± 0.02 |

Errors represent standard errors.

The belowground carbon input from the tree row vegetation ($BEC_{veg,z}$, t C $ha^{-1}$) at a given depth $z$ (m) was described by the following equation:

$$BEC_{veg,z} = \begin{cases} 0.44 \times e^{-3.12 \times z}, & z \leq 1.5 \\ 0, & z > 1.5 \end{cases} \quad (36)$$

### 3.21.6 Organic carbon inputs and SOC stocks: a synthesis from field measurements

Tree rows in the agroforestry system received two times more organic carbon (OC) inputs compared to the control plot (Fig. 3), and 65% more than alleys. GloballyOverall, the agroforestry plot had 41% more OC inputs to the soil than the control plot to 2 m depth (3.80 t C $ha^{-1}$ $yr^{-1}$ compared to 2.69 t C $ha^{-1}$ $yr^{-1}$). In the agroforestry plot, the largest aboveground OC input to the soil comes from the herbaceous vegetation, and not from the trees. In the control plot, 85% of OC inputs are wheat root litters. In the agroforestry plot, root inputs represent 71% of OC inputs in the alleys, and 50% in the tree rows.

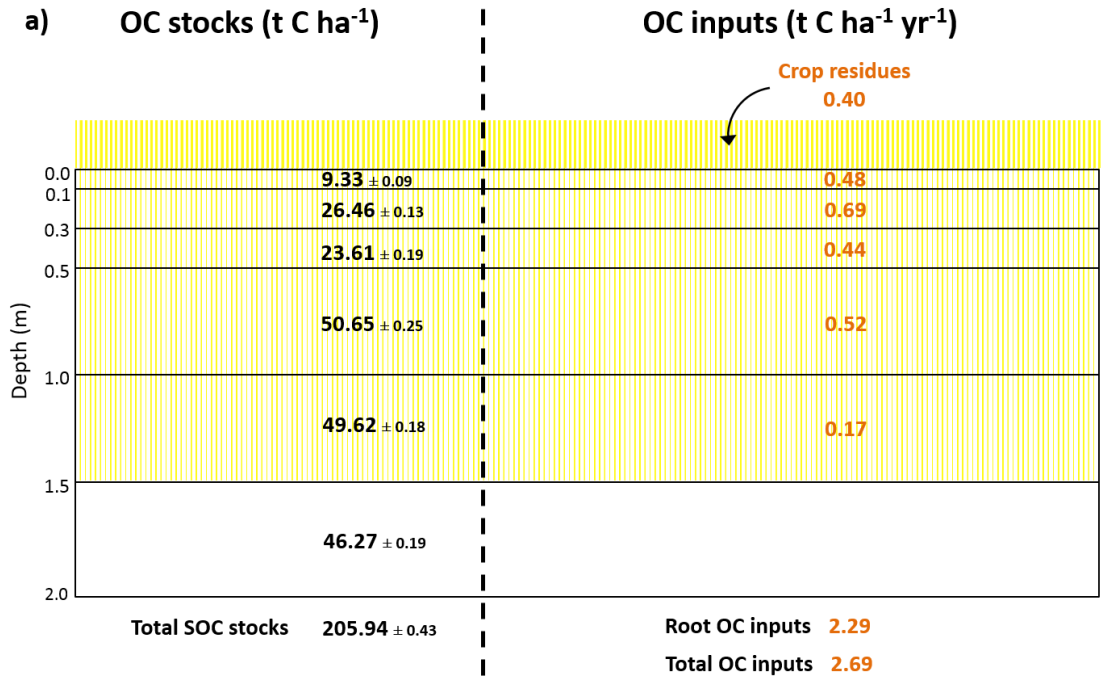
a)
OC stocks (t C ha-1)
OC inputs (t C ha-1 yr-1)
Crop residues
0.40
Depth (m)
0.0
0.1
0.3
0.5
1.0
1.5
2.0
9.33 ± 0.09
26.46 ± 0.13
23.61 ± 0.19
50.65 ± 0.25
49.62 ± 0.18
46.27 ± 0.19
0.48
0.69
0.44
0.52
0.17
Total SOC stocks 205.94 ± 0.43
Root OC inputs 2.29
Total OC inputs 2.69

804

805

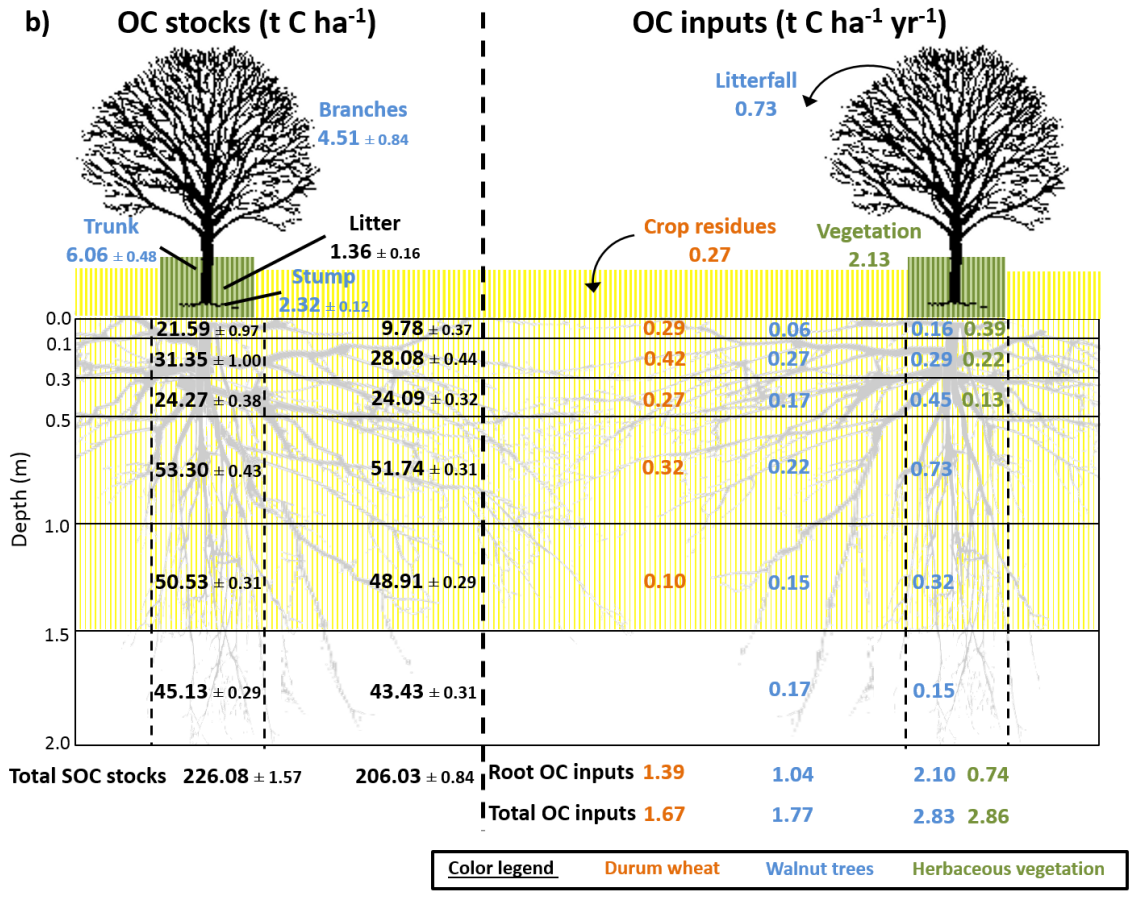
b)
OC stocks (t C ha-1)
OC inputs (t C ha-1 yr-1)
Litterfall
0.73
Branches
4.51 ± 0.84
Trunk
6.06 ± 0.48
Litter
1.36 ± 0.16
Stump
2.32 ± 0.12
Crop residues
0.27
Vegetation
2.13
Depth (m)
0.0
0.1
0.3
0.5
1.0
1.5
2.0
21.59 ± 0.97
31.35 ± 1.00
24.27 ± 0.38
53.30 ± 0.43
50.53 ± 0.31
45.13 ± 0.29
9.78 ± 0.37
28.08 ± 0.44
24.09 ± 0.32
51.74 ± 0.31
48.91 ± 0.29
43.43 ± 0.31
0.29
0.42
0.27
0.32
0.10
0.06
0.27
0.17
0.22
0.15
0.17
0.16 0.39
0.29 0.22
0.45 0.13
0.73
0.32
0.15
Total SOC stocks 226.08 ± 1.57
206.03 ± 0.84
Root OC inputs 1.39
1.04
2.10 0.74
Total OC inputs 1.67
1.77
2.83 2.86
Color legend
Durum wheat
Walnut trees
Herbaceous vegetation

806

**Fig. 3.** Measured soil organic carbon stocks and organic carbon inputs to the soil a) in the agricultural control plot, b) in the 18-year-old agroforestry plot. Associated errors are standard errors. Values are expressed per hectare of land type (control, alley, tree row). To get the values per hectare of agroforestry, data from alley and tree row have to be weighted by their respective surface area (i.e., 84% and 16%, respectively) and then added up. OC: organic carbon; SOC: soil organic carbon. SOC stocks data are issued from Cardinael *et al.*, (2015a), data of tree root OC inputs are combined from Cardinael *et al.*, (2015b) and from Germon *et al.*, (2016).

### 3.~~3~~ 2 HSOC decomposition rate

The soil incubation experiment showed that the HSOC mineralization rate decreased exponentially with depth (Fig. S1) and could be described with:

$$k_{HSOC,z} = 6.114 \times e^{-1.37 \times z} \quad (R^2 = 0.76) \qquad (34)$$

where z is the soil depth (m), and where the $a$ ($yr^{-1}$) coefficient ($a$ = 6.114) was further optimized (Table ~~7~~5).

**Table ~~7~~5.** Summary of optimized model parameters.

| Model parameter | Meaning | Prior range | Posterior values ± variance (prior values) | | |
|---|---|---|---|---|---|
| | | | 2 pools - without *PE* | 2 pools - with *PE* | 3 pools – without *PE* |
| $a$ | coefficient from Eq. (8) of the HSOC decomposition ($yr^{-1}$) | $3.65e^{-6}$-3.65 | $0.01e^{-2} \pm <10^{-4}$ ($0.01e^{-2}$) | $0.01e^{-2} \pm <10^{-4}$ ($0.01e^{-2}$) | - |
| $a_1$ | coefficient from Eq. (8) of the HSOC1 decomposition ($yr^{-1}$) | $3.65e^{-6}$-3.65 | - | - | $0.01e^{-2} \pm <10^{-4}$ ($0.01e^{-2}$) |
| $a_2$ | coefficient from Eq. (8) of the HSOC2 decomposition ($yr^{-1}$) | $3.65e^{-6}$-3.65 | - | - | $0.83e^{-2} \pm 0.17e^{-2}$ ($0.83e^{-2}$) |
| $D$ | diffusion coefficient ($cm^2\ yr^{-1}$) | $1e^{-6}$-1 | $4.62e^{-4} \pm 5.95e^{-4}$ ($9.64e^{-4}$) | $5.63e^{-4} \pm 1.42e^{-4}$ ($9.01e^{-4}$) | $5.24e^{-4} \pm 7.62e^{-4}$ ($9.64e^{-4}$) |
| $A$ | advection rate ($mm\ yr^{-1}$) | $1e^{-6}$-1 | $21.25e^{-4} \pm 5.02e^{-4}$ ($8.54e^{-4}$) | $6.63e^{-4} \pm 2.38e^{-4}$ ($4.27e^{-4}$) | $21.60e^{-4} \pm 2.24e^{-4}$ ($8.54e^{-4}$) |
| $h$ | humification yield | 0.01-1 | $0.32 \pm <10^{-4}$ (0.34) | $0.25 \pm 1.00e^{-4}$ (0.13) | $0.34 \pm 0.03$ (0.34) |
| *PE* | priming coefficient | 0.1-160 | - | $9.66 \pm 1.49$ (102.95) | - |
| $f_1$ | fraction of decomposed FOC entering the HSOC1 pool | 0-1 | - | - | $0.99 \pm 0.18$ (0.86) |
| $f_2$ | fraction of decomposed HSOC1 entering the FOC pool | 0-1 | - | - | $0.94 \pm 1.10e^{-3}$ (0.80) |

The prior range represents the range in which prior values were sampled for the 30 optimizations per model variant. The prior values presented in brackets in the posterior column represent the prior values that minimized the **J(x)** value (Eq. (19)).

## 3.~~4~~ 3 Modeling results

### 3.~~4~~3.1 Optimized parameters and correlation matrix

The optimized parameters and their prior modes are presented in Table ~~7~~5. For the two pools model without priming effect, the most important correlation was observed between *h* and *A* which control the humification and the transport by advection. Concerning the two pools model with priming effect, the most important correlations were observed between *h* and *PE* which controls the effect of the FOC on HSOC decomposition, and between *h* and *A*. *A* and *PE* were also positively correlated (Fig. S2). For the three pools model, $f_1$ and $f_2$ were by definition negatively correlated, but $f_2$ and *A* were also correlated. Considering the method used to optimize the parameters, these important correlation factors hinder the presentation of the model output within an envelope. Therefore, we presented the model results using the optimized parameter without any envelope.

### 3.~~4~~3.2 Modeled SOC stocks

As a reminder, SOC stocks of the agroforestry plot were not part of model calibration (that used the control plot only) but were used here for validation. Observed SOC stocks were not well represented by the two pools model without priming effect, with RMSE ranging from 1.00 to 1.07 kg C $m^{-3}$ (Fig. 4, Table ~~S1~~S2). The model performed better when the priming effect was taken into account, with RMSE ranging from 0.41 to 0.95 kg C $m^{-3}$, and the SOC profile was well described. The representation of SOC stocks was not improved by the inclusion of a third C pool in the model. ~~Globally~~Overall, the two pools model with priming effect was the best one, as shown by the BICs (Fig. 4, Table ~~S1~~S2). For all models, SOC stocks below 1 m depth were better described than above SOC stocks (Table ~~S1~~S2). The spatial distribution of SOC stocks and of additional SOC storage was also well described (Fig. 5), with a very high additional SOC ~~stock~~ storage in the topsoil layer in the tree row. Most modeled SOC storage in

the agroforestry plot was located in the first 0.2 m depth, ~~and~~ but SOC storage was slightly higher in the middle of the alleys than in the alleys close to the tree rows.

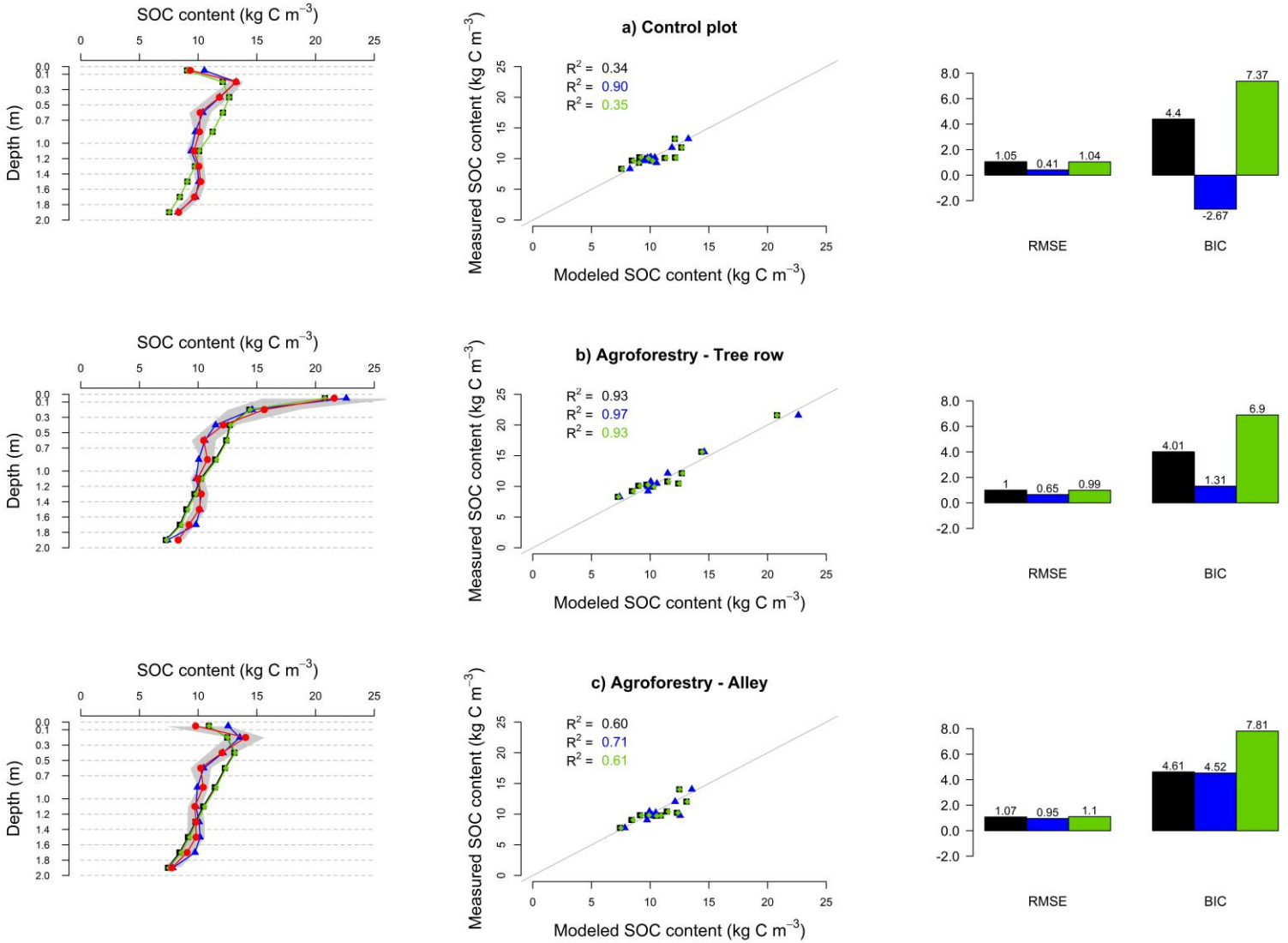
SOC content (kg C m$^{-3}$)
Depth (m)
a) Control plot
$R^2$ = 0.34
$R^2$ = 0.90
$R^2$ = 0.35
Measured SOC content (kg C m$^{-3}$)
Modeled SOC content (kg C m$^{-3}$)
1.05
0.41
1.04
4.4
-2.67
7.37
RMSE
BIC
b) Agroforestry - Tree row
$R^2$ = 0.93
$R^2$ = 0.97
$R^2$ = 0.93
1
0.65
0.99
4.01
1.31
6.9
c) Agroforestry - Alley
$R^2$ = 0.60
$R^2$ = 0.71
$R^2$ = 0.61
1.07
0.95
1.1
4.61
4.52
7.81
Modeled / 2 pools - no PE
Modeled / 2 pools - PE
Modeled / 3 pools - no PE
Measured

854

**Fig. 4.** Measured and modeled soil organic carbon contents (kg C $m^{-3}$) in an agricultural control plot and in an 18-year-old silvoarable system with a two pools model without priming effect (no *PE*), with a two pools model with priming effect (*PE*) and with a three pools model without *PE*. Gray shaded bands represent standard deviations of measured SOC stocks (n=93 in the control, n=40 in the tree rows, and n=60 in the alleys).

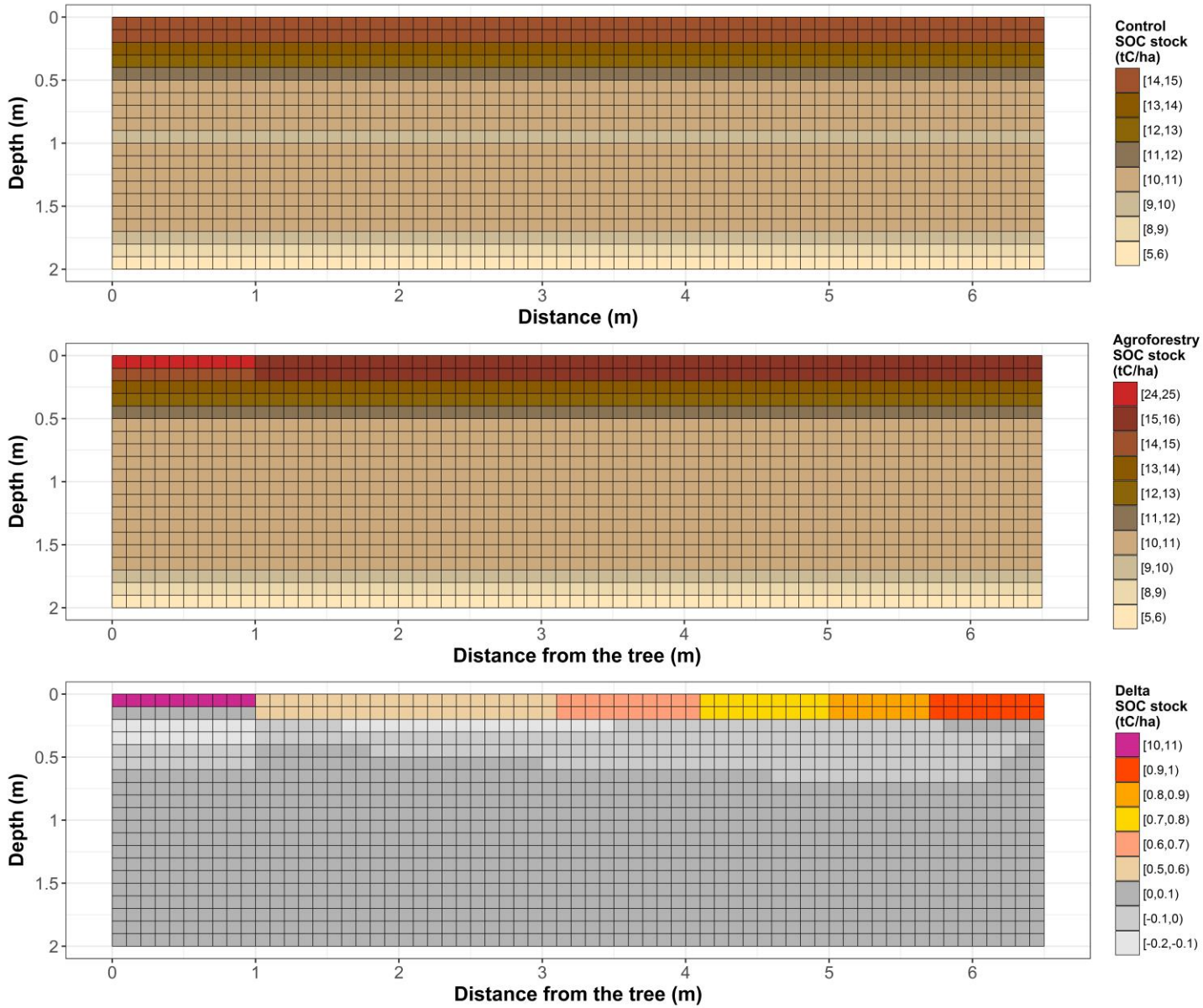
Depth (m)
Distance (m)
Control SOC stock (tC/ha)
[14,15)
[13,14)
[12,13)
[11,12)
[10,11)
[9,10)
[8,9)
[5,6)
Distance from the tree (m)
Agroforestry SOC stock (tC/ha)
[24,25)
[15,16)
[14,15)
[13,14)
[12,13)
[11,12)
[10,11)
[9,10)
[8,9)
[5,6)
Distance from the tree (m)
Delta SOC stock (tC/ha)
[10,11)
[0.9,1)
[0.8,0.9)
[0.7,0.8)
[0.6,0.7)
[0.5,0.6)
[0,0.1)
[-0.1,0)
[-0.2,-0.1)

866

**Fig. 5.** Spatial distribution of control SOC stocks (top), agroforestry SOC stocks (middle), and additional SOC storage (t C $ha^{-1}$) in an 18-year-old silvoarable system compared to an agricultural control plot and represented by the two pools model with priming effect.

### 3.43.3 Antagonist effect of priming on SOC storage

The priming effect increases the decomposition rate when more FOC is available (Fontaine et al., 2007). Therefore, the effect of a C inputs increase on SOC storage in the agroforestry plot might be counterbalanced by priming. With our model we were able to estimate the contribution of each driver on SOC storage. The introduction of priming effect in the model reduced the potential SOC storage due to higher organic inputs in the agroforestry system by 91% in the alley, and by 76% in the tree rows (Fig. 6). The potential effect of OC inputs alone on SOC storage was 49.12 to 62.77 t C $ha^{-1}$, but the effect of priming on SOC storage was -44.89 to -47.67 t C $ha^{-1}$, resulting in a modeled SOC storage of 4.23 t C $ha^{-1}$ in the alley and of 15.09 t C $ha^{-1}$ in the tree row down 2 depth (Fig. 6). The negative effect of priming effect on SOC storage increased with increasing soil depth (Fig. S3).

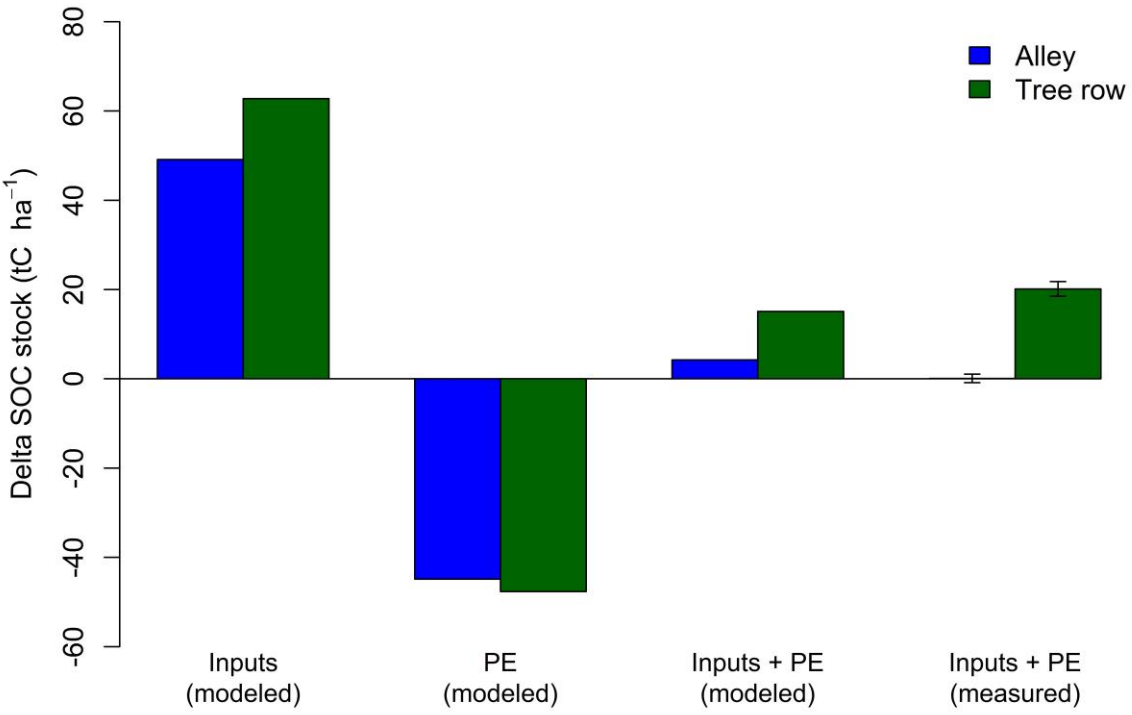


**Fig. 6.** Decoupling the role of C inputs and priming effect (*PE*) on SOC storage in an 18-year-old silvoarable system down 2 m depth. Inputs: only the input effect is modeled; *PE*:

only the priming effect is modeled; Inputs + *PE*: model prediction with both processes taken into account.

# 4 Discussion

## 4.1 OC inputs drive SOC storage in agroforestry systems

Increased SOC stocks in the agroforestry plot compared to the control may be explained either by increased OC inputs, or decreased OC outputs by SOC mineralization, or both. Measured organic carbon inputs to soil were increased by 40% down to 2m depth in the 18-year-old agroforestry plot compared to the control plot. Increased OC inputs in agroforestry systems has been shown in other studies but they were only quantified in the first 20 cm of soil (Oelbermann et al., 2006; Peichl et al., 2006). This study is therefore the first one also quantifying deep OC inputs to soil. In this study and due to a lack of data, soil temperature and soil moisture were considered the same in both plots so that abiotic factors controlling SOC decomposition were identical. Despite these simplifying assumptions on similarities in microclimate but also on vertical transport between the control and the agroforestry system, t~~T~~he model calibrated to the control plot was able to ~~well~~ reproduce SOC stocks in tree rows and alleys and its depth distribution well~~in the agroforestry plot,~~. This strong validation ~~suggesting~~ also suggests that OC inputs is the main driver of SOC storage at this site, and that a ~~decrease of SOC mineralisation due to the agroforestry~~potential effect of agroforestry microclimate on SOC mineralisation is ~~not obvious~~of minor importance. Reduced soil temperature is often observed in agroforestry systems (Clinch et al., 2009; Dubbert et al., 2014), but effect of agroforestry on soil moisture is much more complex. The soil evaporation is reduced under the trees, but water is lost through their transpiration (Ilstedt et al., 2016; Ong and Leakey, 1999), and these effects vary with the distance from the tree (Odhiambo et al., 2001). Moreover, the water infiltration and the water storage can be increased under the trees after a rainy event (Anderson et al.,

2009). Therefore, the effect of agroforestry on soil moisture is variable in time and space, and should be investigated more in details. Interactions between soil temperature and soil moisture on the SOC decomposition are known to be complex (Conant et al., 2011; Moyano et al., 2013; Sierra et al., 2015) and up to now it is not possible to predict the effect of agroforestry microclimate on the SOC decomposition rate. A sensitivity analysis performed on these two boundary conditions showed that the model was not very sensitive to soil temperature and soil moisture (Fig. S4), but the real effect of these two parameters on SOC dynamics under agroforestry systems should be better investigated in future studies. ~~suggesting that the potential changes in soil microclimate in the agroforestry plot are not major drivers of the SOC storage.~~ Furthermore, the SOC decomposition rate could also be modified due to an absence of soil tillage in the tree rows (Balesdent et al., 1990) or to an increased aggregate stability (Udawatta et al., 2008) in the topsoil.

### 4.2 Representation of SOC spatial heterogeneity in agroforestry systems

The lateral spatial heterogeneity of SOC stocks in the agroforestry plot was well described by the two pools model including priming effect, with higher SOC stocks in the tree rows' topsoil than in the alleys. Inputs from the herbaceous vegetation had an important impact on SOC storage in this agroforestry system. The increased SOC stocks in the tree rows were explained in a big part by an important above-ground carbon input (2.13 t C $ha^{-1}$ $yr^{-1}$) by the herbaceous vegetation between trees. This result had already been suggested by Cardinael et al., (2015b) and by Cardinael et al., (2017) who showed that even young agroforestry systems could store SOC in the tree rows while trees are still very small. These "grass strips" indirectly introduced by the tree planting in parallel tree rows have a major impact on SOC stocks of agroforestry systems. The model treated the carbon from this herbaceous litter as an input to the upper layer of the mineral soil, in the same way as inputs by roots. Introduction of nitrogen in the model

could be further tested in order to take into account a lower carbon use efficiency due to a lack of nutrients for microbial growth in this litter. For all models, SOC stocks were better described in the tree rows than in the alleys. In the alleys, the spatial distribution of organic inputs is more complex and thus more difficult to model. The tree root system is influenced by the soil tillage and by the competition with the crop roots, and thus the highest tree fine root density is not observed in the topsoil but in the 0.3-0.5 m soil layer (Cardinael et al., 2015a). In the model, we were not able to represent this specific tree root pattern with commonly used mathematical functions, and tree root profiles were modeled, by default, using a decreasing exponential. Indeed, piecewise linear functions introduce threshold effects not desirable for transport mechanisms, especially diffusion. This simplification could partly explain the model overestimation of SOC stocks in the 0.0-0.1 m layer of the alleys compared to observed data. This result suggests that it could be useful to couple the CARBOSAF model with a model describing root architecture and root growth (Dunbabin et al., 2013; Dupuy et al., 2010), using for instance voxel automata (Mulia et al., 2010). Moreover, the model described a slight increase of SOC stocks in the middle of the alleys than close to the trees in the alleys. This could be explained by the linear equation used to describe the crop yield as a function of the distance from the trees, leading to an overestimation of the crop yield reduction close to the trees. It could also be explained by the formalism used to model leaf litter distribution in the plot. We considered a homogeneous distribution of leaf inputs in the agroforestry plot, which was the case in the last years, but probably not in the first years of the tree growth where leaves might be more concentrated close to the trees (Thevathasan and Gordon, 1997).

The two pools model with priming effect also represented a slight SOC storage in the agroforestry plot below 1.0 m depth, but it was not observed in the field. This could be linked to an overestimation of C input from tree fine root mortality. Indeed, a constant root turnover was considered along the soil profile, but several authors reported a decrease of the root

turnover with increasing soil depth (Germon et al., 2016; Hendrick and Pregitzer, 1996; Joslin et al., 2006). However, the sensitivity analysis showed that the model was not sensitive to this parameter (Fig. S4).

### 4.3 Vertical representation of SOC profiles in models

The best model to represent SOC profiles considered the priming effect. This process can act in two different ways on the shape of SOC profiles. It has a direct effect on the SOC mineralization and it therefore modulates the amount of SOC in each soil layer, creating different SOC gradients. This indirectly affects the mechanisms of C transport within the soil profile, as shown by a modification of transport coefficients in the case of priming effect (Table ~~7~~5). Contrary to what was shown by Cardinael *et al.*, (2015c) in long term bare fallows receiving contrasted organic amendments, the addition of another SOC pool could not surpass the inclusion of priming effect in terms of model performance. Together with Wutzler & Reichstein, (2013) and Guenet *et al.*, (2016), this study therefore suggests that implementing priming effect into SOC models would improve model performances especially when modelling deep SOC profiles.

We considered here the same transport coefficients for the FOC and HSOC pools, but the quality and the size of OC particles are different, potentially leading to various movements in the soil by water fluxes or fauna activity (Lavelle, 1997). Moreover, we considered identical transport parameters in the agroforestry and in the control plot, but the presence of trees could modify soil structure, soil water fluxes (Anderson et al., 2009), and the fauna activity (Price and Gordon, 1999). However, the model was little sensitive to these parameters (Fig. S4). Further study could investigate the role of different transport coefficients on the description of SOC profiles.

### 4.4 Higher OC inputs or a different quality of OC?

The introduction of trees in an agricultural field not only modifies the amount of litter residues, but also their quality. Tree leaves, tree roots, and the herbaceous vegetation from the tree row have different C:N ratios, lignin and cellulose contents than the crop residues. Recent studies showed that plant diversity had a positive impact on SOC storage (Lange et al., 2015; Steinbeiss et al., 2008). One of the hypothesis proposed by the authors is that diverse plant communities result in more active, more abundant and more diverse microbial communities, increasing microbial products that can potentially be stabilized. In our model, litter quality is not related to different SOC pools, but is implicitly taken into account in the FOC decomposition rate, which is weighted by the respective contribution from the different types of OC inputs. To test this, we performed a model run considering that all OC inputs in the agroforestry plot were crop inputs (all FOC decomposition rates equaled wheat decomposition rate), but results were not significantly different from the one presented here. We then consider that changes in litter quality in the agroforestry plot did not significantly influence SOC decomposition rates.

### 4.5 Possible limitation of SOC storage by priming effect

Our modelling results showed that the priming effect could considerably reduce the capacity of soils to store organic carbon. Our study showed that the increase of SOC stocks was not proportional to OC inputs, especially at depth. This result has often been observed in Free Air $CO_2$ Enrichment (FACE) experiments. In these experiments, productivity is usually increased due to $CO_2$ fertilization, but several authors also reported an increase in SOC decomposition but not linearly linked to the productivity increase (van Groenigen et al., 2014; Sulman et al., 2014). In this study, the estimation of the priming effect intensity was possible because most OC inputs to the soil were accurately measured. The modelled intensity of priming effect was very strong, offsetting 75 to 90% of potential SOC storage due to OC inputs. In a long-term

FACE experiment, Carney *et al.*, (2007) also found that SOC decreased due to priming effect, offsetting 52% of additional carbon accumulated in aboveground and coarse root biomass. The priming effect intensity also relies on nutrient availability (Zhang et al., 2013). In agroforestry systems, tree roots can intercept leached nitrate below the crop rooting zone (Andrianarisoa et al., 2016), reducing nutrient availability. This beneficial ecosystem service could indirectly increase the priming effect intensity in deep soil layers.

However, this strong intensity could also partially be linked to the formalism used to simulate priming effect. This formalism assumes that there is no mineralisation of the SOC in the absence of fresh OC inputs (no basal respiration). This is a strong hypothesis, but this situation never occurs since the FOC pool is never empty (data not shown). In the alleys and below the maximum rooting depth of crops, there are no direct inputs of FOC, but OC is transported in these deep layers due to transport mechanisms. However, further studies could study the impact of the priming effect formalism on the estimation of its intensity by using explicit microbial biomass for instance (Blagodatsky et al., 2010; Perveen et al., 2014).

Finally, root exudates were not quantified in this study. Several authors showed that they could induce strong priming effects (Bengtson et al., 2012; Keiluweit et al., 2015), but root exudates are also a source of labile carbon, potentially contributing to stable SOC (Cotrufo et al., 2013). These opposing effects of root exudates on SOC should be further investigated, especially concerning the deep roots in agroforestry systems.

## 5 Conclusions

We proposed the first model that simulates soil organic carbon dynamics in agroforestry accounting for both the whole soil profile and the lateral spatial heterogeneity in agroforestry plots. ~~This~~ The two pools model with priming effect described reasonably well the measured SOC stocks after 18 years of agroforestry and SOC distributions with depth. It showed that the

increased inputs of fresh biomass to soil in the agroforestry system explained the observed additional SOC storage and suggested priming effect as a process controlling SOC stocks in the presence of trees. This study points out at processes that may be modified by deep rooting trees and deserve further studies given their potential effects on SOC dynamics, such as additional inputs of C as roots exudates, or altered soil structure leading to modified SOC transport rates.

## 6 Data availability

The data and the model are freely available upon request and can be obtained by contacting the author (remi.cardinael@cirad.fr).

## Information about the Supplement

The Supplement includes the walnut tree fine root biomass (Table S1), the different model performances (Table S2~~1~~), the potential SOC decomposition rate as a function of soil depth (Fig. S1), the correlation matrix of optimized parameters (Fig. ~~8~~S2), the decoupling of OC inputs and priming effect as a function of soil depth (Fig. S3), and a sensitivity analysis of the model (Fig. S4).

*Acknowledgments.*

This study was financed by the French Environment and Energy Management Agency (ADEME), following a call for proposals as part of the REACCTIF program (Research on Climate Change Mitigation in Agriculture and Forestry). This work was part of the funded project AGRIPSOL (Agroforestry for Soil Protection, 1260C0042), coordinated by Agroof. Rémi Cardinael was supported both by ADEME and by La Fondation de France. We thank the farmer, Mr Breton, who allowed us to sample in his field. We are very grateful to our colleagues for their work in the field since the tree planting, especially Jean-François Bourdoncle, Myriam

Dauzat, Lydie Dufour, Jonathan Mineau, Alain Sellier and Benoit Suard. We thank colleagues and students who helped us for measurements in the field or in the laboratory, especially Daniel Billiou, Cyril Girardin, Patricia Mahafaka, Agnès Martin, Valérie Pouteau, Alexandre Rosa, and Manon Villeneuve. Finally, we would like to thank Jérôme Balesdent and Pierre Barré for their valuable comments on the modeling part of this work.

## References

Ahrens, B., Braakhekke, M. C., Guggenberger, G., Schrumpf, M. and Reichstein, M.: Contribution of sorption, DOC transport and microbial interactions to the $^{14}C$ age of a soil organic carbon profile: Insights from a calibrated process model, Soil Biol. Biochem., 88, 390–402, 2015.

Albrecht, A. and Kandji, S. T.: Carbon sequestration in tropical agroforestry systems, Agric. Ecosyst. Environ., 99, 15–27, 2003.

Anderson, S. H., Udawatta, R. P., Seobi, T. and Garrett, H. E.: Soil water content and infiltration in agroforestry buffer strips, Agrofor. Syst., 75(1), 5–16, 2009.

Andrianarisoa, K., Dufour, L., Bienaime, S., Zeller, B. and Dupraz, C.: The introduction of hybrid walnut trees (*Juglans nigra* x *regia* cv. NG23) into cropland reduces soil mineral N content in autumn in southern France, Agrofor. Syst., 90, 193–205, 2016.

Baisden, W. T. and Parfitt, R. L.: Bomb $^{14}C$ enrichment indicates decadal C pool in deep soil?, Biogeochemistry, 85, 59–68, 2007.

Baisden, W. T., Amundson, R., Brenner, D. L., Cook, A. C., Kendall, C. and Harden, J. W.: A multiisotope C and N modeling analysis of soil organic matter turnover and transport as a function of soil depth in a California annual grassland soil chronosequence, Global Biogeochem. Cycles, 16, 82-1-82–26, 2002.

1082 Balandier, P. and Dupraz, C.: Growth of widely spaced trees. A case study from young
1083 agroforestry plantations in France, Agrofor. Syst., 43, 151–167, 1999.

1084 Balesdent, J., Mariotti, A. and Boisgontier, D.: Effect of tillage on soil organic carbon
1085 mineralization estimated from 13C abundance in maize fields, J. Soil Sci., 41, 587–596, 1990.

1086 Bambrick, A. D., Whalen, J. K., Bradley, R. L., Cogliastro, A., Gordon, A. M., Olivier, A. and
1087 Thevathasan, N. V: Spatial heterogeneity of soil organic carbon in tree-based intercropping
1088 systems in Quebec and Ontario, Canada, Agrofor. Syst., 79, 343–353, 2010.

1089 Bengtson, P., Barker, J. and Grayston, S. J.: Evidence of a strong coupling between root
1090 exudation, C and N availability, and stimulated SOM decomposition caused by rhizosphere
1091 priming effects, Ecol. Evol., 2(8), 1843–1852, 2012.

1092 Blagodatsky, S., Blagodatskaya, E., Yuyukina, T. and Kuzyakov, Y.: Model of apparent and
1093 real priming effects: Linking microbial activity with soil organic matter decomposition, Soil
1094 Biol. Biochem., 42, 1275–1283, 2010.

1095 Braakhekke, M. C., Beer, C., Hoosbeek, M. R., Reichstein, M., Kruijt, B., Schrumpf, M. and
1096 Kabat, P.: SOMPROF: A vertically explicit soil organic matter model, Ecol. Modell., 222,
1097 1712–1730, 2011.

1098 Bruun, S., Christensen, B. T., Thomsen, I. K., Jensen, E. S. and Jensen, L. S.: Modeling vertical
1099 movement of organic matter in a soil incubated for 41 years with $^{14}C$ labeled straw, Soil Biol.
1100 Biochem., 39, 368–371, 2007.

1101 Burgess, P. J., Incoll, L. D., Corry, D. T., Beaton, A. and Hart, B. J.: Poplar (*Populus* spp)
1102 growth and crop yields in a silvoarable experiment at three lowland sites in England, Agrofor.
1103 Syst., 63, 157–169, 2004.

1104 Cardinael, R., Mao, Z., Prieto, I., Stokes, A., Dupraz, C., Kim, J. H. and Jourdan, C.:
1105 Competition with winter crops induces deeper rooting of walnut trees in a Mediterranean alley

cropping agroforestry system, Plant Soil, 391, 219–235, 2015a.

Cardinael, R., Chevallier, T., Barthès, B. G., Saby, N. P. ., Parent, T., Dupraz, C., Bernoux, M. and Chenu, C.: Impact of alley cropping agroforestry on stocks, forms and spatial distribution of soil organic carbon - A case study in a Mediterranean context, Geoderma, 259–260, 288–299, 2015b.

Cardinael, R., Eglin, T., Guenet, B., Neill, C., Houot, S. and Chenu, C.: Is priming effect a significant process for long-term SOC dynamics? Analysis of a 52-years old experiment, Biogeochemistry, 123, 203–219, 2015c.

Cardinael, R., Chevallier, T., Cambou, A., Béral, C., Barthès, B. G., Dupraz, C., Durand, C., Kouakoua, E. and Chenu, C.: Increased soil organic carbon stocks under agroforestry: A survey of six different sites in France, Agric. Ecosyst. Environ., 236, 243–255, 2017.

Carney, K. M., Hungate, B. A., Drake, B. G. and Megonigal, J. P.: Altered soil microbial community at elevated CO2 leads to loss of soil carbon, PNAS, 104, 4990–4995, 2007.

Charbonnier, F., le Maire, G., Dreyer, E., Casanoves, F., Christina, M., Dauzat, J., Eitel, J. U. H., Vaast, P., Vierling, L. a. and Roupsard, O.: Competition for light in heterogeneous canopies: Application of MAESTRA to a coffee (Coffea arabica L.) agroforestry system, Agric. For. Meteorol., 181, 152–169, 2013.

Chaudhry, A. K., Khan, G. S., Siddiqui, M. T., Akhtar, M. and Aslam, Z.: Effect of arable crops on the growth of poplar (Populus deltoides) tree in agroforestry system, Pakistan J. Agric. Sci., 40, 82–85, 2003.

Chifflot, V., Bertoni, G., Cabanettes, A. and Gavaland, A.: Beneficial effects of intercropping on the growth and nitrogen status of young wild cherry and hybrid walnut trees, Agrofor. Syst., 66, 13–21, 2006.

Clinch, R. L., Thevathasan, N. V., Gordon, A. M., Volk, T. A. and Sidders, D.: Biophysical

1130 interactions in a short rotation willow intercropping system in southern Ontario, Canada, Agric.
1131 Ecosyst. Environ., 131, 61–69, 2009.

1132 Conant, R. T., Ryan, M. G., Ågren, G. I., Birge, H. E., Davidson, E. A., Eliasson, P. E., Evans,
1133 S. E., Frey, S. D., Giardina, C. P., Hopkins, F. M., Hyvönen, R., Kirschbaum, M. U. F.,
1134 Lavallee, J. M., Leifeld, J., Parton, W. J., Megan Steinweg, J., Wallenstein, M. D., Martin
1135 Wetterstedt, J. Å. and Bradford, M. A.: Temperature and soil organic matter decomposition
1136 rates - synthesis of current knowledge and a way forward, Glob. Chang. Biol., 17, 3392–3404,
1137 2011.

1138 Cotrufo, M. F., Wallenstein, M. D., Boot, C. M., Denef, K. and Paul, E.: The Microbial
1139 Efficiency-Matrix Stabilization (MEMS) framework integrates plant litter decomposition with
1140 soil organic matter stabilization: do labile plant inputs form stable soil organic matter?, Glob.
1141 Chang. Biol., 19, 988–95, 2013.

1142 Davidson, E. A. and Janssens, I. A.: Temperature sensitivity of soil carbon decomposition and
1143 feedbacks to climate change, Nature, 440, 165–173, 2006.

1144 Dimassi, B., Cohan, J.-P., Labreuche, J. and Mary, B.: Changes in soil carbon and nitrogen
1145 following tillage conversion in a long-term experiment in Northern France, Agric. Ecosyst.
1146 Environ., 169, 12–20, 2013.

1147 Dubbert, M., Mosena, A., Piayda, A., Cuntz, M., Correia, A. C., Pereira, J. S. and Werner, C.:
1148 Influence of tree cover on herbaceous layer development and carbon and water fluxes in a
1149 Portuguese cork-oak woodland, Acta Oecologica, 59, 35–45, 2014.

1150 Dufour, L., Metay, A., Talbot, G. and Dupraz, C.: Assessing Light Competition for Cereal
1151 Production in Temperate Agroforestry Systems using Experimentation and Crop Modelling, J.
1152 Agron. Crop Sci., 199, 217–227, 2013.

1153 Dunbabin, V. M., Postma, J. A., Schnepf, A., Pagès, L., Javaux, M., Wu, L., Leitner, D., Chen,

Y. L., Rengel, Z. and Diggle, A. J.: Modelling root-soil interactions using three-dimensional models of root growth, architecture and function, Plant Soil, 372, 93–124, 2013.

Dupuy, L., Gregory, P. J. and Bengough, A. G.: Root growth models: Towards a new generation of continuous approaches, J. Exp. Bot., 61, 2131–2143, 2010.

Duursma, R. . and Medlyn, B. .: MAESPA: a model to study interactions between water limitation, environmental drivers and vegetation function at tree and stand levels, with an example application to [$CO_2$] × drought interactions, Geosci. Model Dev., 5, 919–940, 2012.

Eilers, K. G., Debenport, S., Anderson, S. and Fierer, N.: Digging deeper to find unique microbial communities: The strong effect of depth on the structure of bacterial and archaeal communities in soil, Soil Biol. Biochem., 50, 58–65, 2012.

Eissenstat, D. M. and Yanai, R. D.: The Ecology of Root Lifespan, Adv. Ecol. Res., 27, 1–60, 1997.

Ellert, B. H. and Bettany, J. R.: Calculation of organic matter and nutrients stored in soils under contrasting management regimes, Can. J. Soil Sci., 75, 529–538, 1995.

Elzein, A. and Balesdent, J.: Mechanistic simulation of vertical distribution of carbon concentrations and residence times in soils, Soil Sci. Soc. Am. J., 59, 1328–1335, 1995.

Fierer, N., Schimel, J. P. and Holden, P. A.: Variations in microbial community composition through two soil depth profiles, Soil Biol. Biochem., 35, 167–176, 2003.

Fontaine, S., Barot, S., Barré, P., Bdioui, N., Mary, B. and Rumpel, C.: Stability of organic carbon in deep soil layers controlled by fresh carbon supply, Nature, 450, 277–281, 2007.

Germon, A., Cardinael, R., Prieto, I., Mao, Z., Kim, J. H., Stokes, A., Dupraz, C., Laclau, J.-P. and Jourdan, C.: Unexpected phenology and lifespan of shallow and deep fine roots of walnut trees grown in a silvoarable Mediterranean agroforestry system, Plant Soil, 401, 409–426, 2016.

Graves, A. R., Burgess, P. J., Palma, J. H. N., Herzog, F., Moreno, G., Bertomeu, M., Dupraz,

C., Liagre, F., Keesman, K., van der Werf, W., de Nooy, a. K. and van den Briel, J. P.: Development and application of bio-economic modelling to compare silvoarable, arable, and forestry systems in three European countries, Ecol. Eng., 29, 434–449, 2007.

Graves, A. R., Burgess, P. J., Palma, J., Keesman, K. J., van der Werf, W., Dupraz, C., van Keulen, H., Herzog, F. and Mayus, M.: Implementation and calibration of the parameter-sparse Yield-SAFE model to predict production and land equivalent ratio in mixed tree and crop systems under two contrasting production situations in Europe, Ecol. Modell., 221, 1744–1756, 2010.

van Groenigen, K. J., Qi, X., Osenberg, C. W., Luo, Y. and Hungate, B. A.: Faster decomposition under increased atmospheric CO2 limits soil carbon storage, Science, 344, 508–509, 2014.

Guenet, B., Eglin, T., Vasilyeva, N., Peylin, P., Ciais, P. and Chenu, C.: The relative importance of decomposition and transport mechanisms in accounting for soil organic carbon profiles, Biogeosciences, 10, 2379–2392, 2013.

Guenet, B., Moyano, F. E., Peylin, P., Ciais, P. and Janssens, I. A.: Towards a representation of priming on soil carbon decomposition in the global land biosphere model ORCHIDEE (version 1.9.5.2), Geosci. Model Dev., 9, 841–855, 2016.

Haile, S. G., Nair, V. D. and Nair, P. K. R.: Contribution of trees to carbon storage in soils of silvopastoral systems in Florida, USA, Glob. Chang. Biol., 16, 427–438, 2010.

Hendrick, R. L. and Pregitzer, K. S.: Temporal and depth-related patterns of fine root dynamics in northern hardwood forests, J. Ecol., 84, 167–176, 1996.

Howlett, D. S., Moreno, G., Mosquera Losada, M. R., Nair, P. K. R. and Nair, V. D.: Soil carbon storage as influenced by tree cover in the Dehesa cork oak silvopasture of central-western Spain, J. Environ. Monit., 13, 1897–904, 2011.

Ilstedt, U., Bargués Tobella, A., Bazié, H. R., Bayala, J., Verbeeten, E., Nyberg, G., Sanou, J., Benegas, L., Murdiyarso, D., Laudon, H., Sheil, D. and Malmer, A.: Intermediate tree cover can maximize groundwater recharge in the seasonally dry tropics, Sci. Rep., 6, 21930, 2016.

IUSS Working Group WRB: World Reference Base for Soil Resources 2006, first update 2007. World Soil Resources Reports No. 103. FAO, Rome., 2007.

Jobbagy, E. G. and Jackson, R. B.: The vertical distribution of soil organic carbon and its relation to climate and vegetation, Ecol. Appl., 10, 423–436, 2000.

Joslin, J. D., Gaudinski, J. B., Torn, M. S., Riley, W. J. and Hanson, P. J.: Fine-root turnover patterns and their relationship to root diameter and soil depth in a $^{14}C$-labeled hardwood forest, New Phytol., 172, 523–535, 2006.

Kätterer, T., Bolinder, M. A., Andrén, O., Kirchmann, H. and Menichetti, L.: Roots contribute more to refractory soil organic matter than above-ground crop residues, as revealed by a long-term field experiment, Agric. Ecosyst. Environ., 141, 184–192, 2011.

Keiluweit, M., Bougoure, J. J., Nico, P. S., Pett-Ridge, J., Weber, P. K. and Kleber, M.: Mineral protection of soil carbon counteracted by root exudates, Nat. Clim. Chang., 5, 588–595, 2015.

Kim, D.-G., Kirschbaum, M. U. F. and Beedy, T. L.: Carbon sequestration and net emissions of $CH_4$ and $N_2O$ under agroforestry: Synthesizing available data and suggestions for future studies, Agric. Ecosyst. Environ., 226, 65–78, 2016.

Koarashi, J., Hockaday, W. C., Masiello, C. A. and Trumbore, S. E.: Dynamics of decadally cycling carbon in subsurface soils, J. Geophys. Res., 117, 1–13, 2012.

Koven, C. D., Riley, W. J., Subin, Z. M., Tang, J. Y., Torn, M. S., Collins, W. D., Bonan, G. B., Lawrence, D. M. and Swenson, S. C.: The effect of vertically resolved soil biogeochemistry and alternate soil C and N models on C dynamics of CLM4, Biogeosciences, 10, 7109–7131, 2013.

Lange, M., Eisenhauer, N., Sierra, C. A., Bessler, H., Engels, C., Griffiths, R. I., Mellado-Vázquez, P. G., Malik, A. A., Roy, J., Scheu, S., Steinbeiss, S., Thomson, B. C., Trumbore, S. E. and Gleixner, G.: Plant diversity increases soil microbial activity and soil carbon storage, Nat. Commun., 6, 6707, 2015.

Lavelle, P.: Faunal activities and soil processes: adaptative strategy that determine ecosystem function., 1997.

Li, F., Meng, P., Fu, D. and Wang, B.: Light distribution, photosynthetic rate and yield in a Paulownia-wheat intercropping system in China, Agrofor. Syst., 74, 163–172, 2008.

Lorenz, K. and Lal, R.: Soil organic carbon sequestration in agroforestry systems. A review, Agron. Sustain. Dev., 34, 443–454, 2014.

Luedeling, E., Smethurst, P. J., Baudron, F., Bayala, J., Huth, N. I., van Noordwijk, M., Ong, C. K., Mulia, R., Lusiana, B., Muthuri, C. and Sinclair, F. L.: Field-scale modeling of tree-crop interactions: Challenges and development needs, Agric. Syst., 142, 51–69, 2016.

Manzoni, S., Piñeiro, G., Jackson, R. B., Jobbágy, E. G., Kim, J. H. and Porporato, A.: Analytical models of soil and litter decomposition: Solutions for mass loss and time-dependent decay rates, Soil Biol. Biochem., 50, 66–76, 2012.

Mead, R. and Willey, R. W.: The concept of a “land equivalent ratio” and advantages in yields from intercropping, Exp. Agric., 16, 217–228, 1980.

Moreno, G., Obrador, J. J., Cubera, E. and Dupraz, C.: Fine root distribution in Dehesas of central-western Spain, Plant Soil, 277, 153–162, 2005.

Moyano, F. E., Vasilyeva, N., Bouckaert, L., Cook, F., Craine, J., Curiel Yuste, J., Don, a., Epron, D., Formanek, P., Franzluebbers, a., Ilstedt, U., Kätterer, T., Orchard, V., Reichstein, M., Rey, A., Ruamps, L., Subke, J. A., Thomsen, I. K. and Chenu, C.: The moisture response of soil heterotrophic respiration: Interaction with soil properties, Biogeosciences, 9, 1173–

1182, 2012.

Moyano, F. E., Manzoni, S. and Chenu, C.: Responses of soil heterotrophic respiration to moisture availability: An exploration of processes and models, Soil Biol. Biochem., 59, 72–85, 2013.

Mulia, R. and Dupraz, C.: Unusual fine root distributions of two deciduous tree species in southern France: What consequences for modelling of tree root dynamics?, Plant Soil, 281, 71–85, 2006.

Mulia, R., Dupraz, C. and van Noordwijk, M.: Reconciling root plasticity and architectural ground rules in tree root growth models with voxel automata, Plant Soil, 337, 77–92, 2010.

Nair, P. K.: An introduction to agroforestry, Kluwer Academic Publishers, Dordrecht, The Netherlands., 1993.

Nair, P. K. R.: Classification of agroforestry systems, Agrofor. Syst., 3, 97–128, 1985.

van Noordwijk, M. and Lusiana, B.: WaNuLCAS, a model of water, nutrient and light capture in agroforestry systems, Agrofor. Syst., 43, 217–242, 1999.

Odhiambo, H. O., Ong, C. K., Deans, J. D., Wilson, J., Khan, A. A. H. and Sprent, J. I.: Roots, soil water and crop yield: Tree crop interactions in a semi-arid agroforestry system in Kenya, Plant Soil, 235, 221–233, 2001.

Oelbermann, M. and Voroney, R. P.: And evaluation of the century model to predict soil organic carbon: examples from Costa Rica and Canada, Agrofor. Syst., 82, 37–50, 2011.

Oelbermann, M., Voroney, R. P. and Gordon, A. M.: Carbon sequestration in tropical and temperate agroforestry systems: a review with examples from Costa Rica and southern Canada, Agric. Ecosyst. Environ., 104, 359–377, 2004.

Oelbermann, M., Voroney, R. P., Thevathasan, N. V., Gordon, A. M., Kass, D. C. L. and Schlönvoigt, A. M.: Soil carbon dynamics and residue stabilization in a Costa Rican and

1274 southern Canadian alley cropping system, Agrofor. Syst., 68, 27–36, 2006.

1275 Ong, C. K. and Leakey, R. R. B.: Why tree-crop interactions in agroforestry appear at odds with
1276 tree-grass interactions in tropical savannahs, Agrofor. Syst., 45, 109–129, 1999.

1277 Parton, W. J., Schimel, D. S., Cole, C. V and Ojima, D. S.: Analysis of factors controlling soil
1278 organic matter levels in great plains grasslands, Soil Sci. Soc. Am. J., 51, 1173–1179, 1987.

1279 Peichl, M., Thevathasan, N. V, Gordon, A. M., Huss, J. and Abohassan, R. A.: Carbon
1280 sequestration potentials in temperate tree-based intercropping systems, southern Ontario,
1281 Canada, Agrofor. Syst., 66, 243–257, 2006.

1282 Perveen, N., Barot, S., Alvarez, G., Klumpp, K., Martin, R., Rapaport, A., Herfurth, D.,
1283 Louault, F. and Fontaine, S.: Priming effect and microbial diversity in ecosystem functioning
1284 and response to global change: A modeling approach using the SYMPHONY model, Glob.
1285 Chang. Biol., 20, 1174–1190, 2014.

1286 Price, G. W. and Gordon, A. M.: Spatial and temporal distribution of earthworms in a temperate
1287 intercropping system in southern Ontario, Canada, Agrofor. Syst., 44, 141–149, 1999.

1288 Prieto, I., Roumet, C., Cardinael, R., Kim, J., Maeght, J.-L., Mao, Z., Portillo, N.,
1289 Thammahacksa, C., Dupraz, C., Jourdan, C., Pierret, A., Roupsard, O. and Stokes, A.: Root
1290 functional parameters along a land-use gradient: evidence of a community-level economics
1291 spectrum, J. Ecol., 103, 361–373, 2015.

1292 Prieto, I., Stokes, A. and Roumet, C.: Root functional parameters predict fine root
1293 decomposability at the community level, J. Ecol., 104, 725–733, 2016.

1294 R Development Core Team: R: A language and environment for statistical computing, 2013.

1295 Rasse, D. P., Mulder, J., Moni, C. and Chenu, C.: Carbon turnover kinetics with depth in a
1296 French loamy soil, Soil Sci. Soc. Am. J., 70, 2097–2105, 2006.

1297 Salomé, C., Nunan, N., Pouteau, V., Lerch, T. Z. and Chenu, C.: Carbon dynamics in topsoil

1298 and in subsoil may be controlled by different regulatory mechanisms, Glob. Chang. Biol., 16,
1299 416–426, 2010.

1300 Santaren, D., Peylin, P., Viovy, N. and Ciais, P.: Optimizing a process-based ecosystem model
1301 with eddy-covariance flux measurements: A pine forest in southern France, Global
1302 Biogeochem. Cycles, 21, 1–15, 2007.

1303 Shahzad, T., Chenu, C., Genet, P., Barot, S., Perveen, N., Mougin, C. and Fontaine, S.:
1304 Contribution of exudates, arbuscular mycorrhizal fungi and litter depositions to the rhizosphere
1305 priming effect induced by grassland species, Soil Biol. Biochem., 80, 146–155, 2015.

1306 Sierra, C. A., Trumbore, S. E., Davidson, E. A., Vicca, S. and Janssens, I.: Sensitivity of
1307 decomposition rates of soil organic matter with respect to simultaneous changes in temperature
1308 and moisture, J. Adv. Model. Earth Syst., 7, 335–356, 2015.

1309 Soetaert, K., Petzoldt, T. and Woodrow Setzer, R.: Solving Differential Equations in R:
1310 Package deSolve, J. Stat. Softw., 33, 1–25, 2010.

1311 Somarriba, E.: Revisiting the past: an essay on agroforestry definition, Agrofor. Syst., 19(3),
1312 233–240, 1992.

1313 Steinbeiss, S., Beßler, H., Engels, C., Temperton, V. M., Buchmann, N., Roscher, C.,
1314 Kreutziger, Y., Baade, J., Habekost, M. and Gleixner, G.: Plant diversity positively affects
1315 short-term soil carbon storage in experimental grasslands, Glob. Chang. Biol., 14, 2937–2949,
1316 2008.

1317 Sulman, B. N., Phillips, R. P., Oishi, A. C., Shevliakova, E. and Pacala, S. W.: Microbe-driven
1318 turnover offsets mineral-mediated storage of soil carbon under elevated $CO_2$, Nat. Clim.
1319 Chang., 4, 1099–1102, 2014.

1320 Taghizadeh-Toosi, A., Christensen, B. T., Hutchings, N. J., Vejlin, J., Kätterer, T., Glendining,
1321 M. and Olesen, J. E.: C-TOOL: A simple model for simulating whole-profile carbon storage in

temperate agricultural soils, Ecol. Modell., 292, 11–25, 2014.

Talbot, G.: L'intégration spatiale et temporelle du partage des ressources dans un système agroforestier noyers-céréales: une clef pour en comprendre la productivité ?, PhD Dissertation, Université Montpellier II., 2011.

Tarantola, A.: Inverse problem theory: methods for data fitting and model parameter estimation, edited by Elsevier., 1987.

Tarantola, A.: Inverse Problem Theory and Methods for Model Parameter Estimation, edited by SIAM., 2005.

Thevathasan, N. V. and Gordon, A. M.: Poplar leaf biomass distribution and nitrogen dynamics in a poplar-barley intercropped system in southern Ontario, Canada, Agrofor. Syst., 37, 79–90, 1997.

Udawatta, R. P., Kremer, R. J., Adamson, B. W. and Anderson, S. H.: Variations in soil aggregate stability and enzyme activities in a temperate agroforestry practice, Appl. Soil Ecol., 39, 153–160, 2008.

Virto, I., Barré, P., Burlot, A. and Chenu, C.: Carbon input differences as the main factor explaining the variability in soil organic C storage in no-tilled compared to inversion tilled agrosystems, Biogeochemistry, 108, 17–26, 2012.

van der Werf, W., Keesman, K., Burgess, P., Graves, A., Pilbeam, D., Incoll, L. D., Metselaar, K., Mayus, M., Stappers, R., van Keulen, H., Palma, J. and Dupraz, C.: Yield-SAFE: A parameter-sparse, process-based dynamic model for predicting resource capture, growth, and production in agroforestry systems, Ecol. Eng., 29, 419–433, 2007.

Wutzler, T. and Reichstein, M.: Colimitation of decomposition by substrate and decomposers - a comparison of model formulations, Biogeosciences, 5, 749–759, 2008.

Wutzler, T. and Reichstein, M.: Priming and substrate quality interactions in soil organic matter

models, Biogeosciences, 10, 2089–2103, 2013.

Yin, R. and He, Q.: The spatial and temporal effects of paulownia intercropping: The case of northern China, Agrofor. Syst., 37, 91–109, 1997.

Zhang, W., Wang, X. and Wang, S.: Addition of external organic carbon and native soil organic carbon decomposition: a meta-analysis., PLoS One, 8, e54779, 2013.